Synthesis and Characterization of Deep Eutectic Solvents (DESs)

by

Siti Nor Afifah Binti Rosmi

16775

Dissertation submitted in partial fulfilment of

the requirements for the

Bachelor of Engineering (Hons)

(Chemical Engineering)

MAY 2015

Universiti Teknologi PETRONAS,

32610 Bandar Seri Iskandar,

Perak Darul Ridzuan.

CERTIFICATION OF APPROVAL

Synthesis and Characterization of Deep Eutectic Solvents (DESs)

by

Siti Nor Afifah Binti Rosmi

16775

A project dissertation submitted to the

Chemical Engineering Programme

Universiti Teknologi PETRONAS

in partial fulfilment of the requirement for the

BACHELOR OF ENGINEERING (Hons)

(CHEMICAL ENGINEERING)

Approved by,

_____

Prof. Dr. Thanabalan Murugesan

UNIVERSITI TEKNOLOGI PETRONAS

BANDAR SERI ISKANDAR, PERAK

May 2015

CERTIFICATION OF ORIGINALITY

This is to certify that I am responsible for the work submitted in this project, that the original work is my own except as specified in the references and acknowledgements, and that the original work contained herein have not been undertaken or done by unspecified sources or persons.

_____

SITI NOR AFIFAH BINTI ROSMI

ABSTRACT

It is broadly known that carbon dioxide (CO_2) is one of the major greenhouse gas (GHG) contributors. There have been many researches and studies conducted in order to come up with the most effective method for CO_2 capture. For this project, variety of new DESs is being synthesized and the prepared DESs are chosen based on the structure of salts and the HBD. Materials selected for this project are potassium carbonate, sodium acetate as salt, ethylene glycol, and levulinic acid as hydrogen bond donor (HBD).

This project is an experimental based project and the time period given, the experimental work covers the physical properties analysis which consists of determination of the freezing point, density, viscosity, and refractive index over different pressure, temperature and molar ratio of the mixtures. Densities, viscosities and refractive index of sample formed decrease with an increase of temperature and an increase of HBD content. The temperature dependence of densities and refractive indexes for sample are correlated by an empirical linear function, and the viscosities are fitted using Vogel-Tamman-Flucher (VTF) equation. In this project, Peng-Robinson (PR) Equation of State (EoS) is used to measure the solubility of CO_2. The CO_2 solubility of the studied DESs increases as the pressure and HBD content increases.

ACKNOWLEDGEMENT

TABLE OF CONTENTS

LIST OF FIGURES

LIST OF TABLES

CHAPTER 1

INTRODUCTION

1.1   Background of Study

It is widely acceptable that global warming is occurring. Many scientists believe that the major cause is the emission of greenhouse gases (GHGs), such as carbon dioxide (CO_2), nitrous oxide (N_2O) and methane (CH_4), into the atmosphere. Among these GHGs, CO_2 is the largest contributor in regards to its amount present in the atmosphere contributing to about 60% of the global warming effects [1].

CO_2 emissions can also be broken down by the economic activities that lead to their production [2]. The major sources of CO_2 emission are showed in Figure 1.1. The burning of coal, natural gas, and oil for electricity and heat is the largest single source of CO_2 emissions. Besides, CO_2 emissions also arise from industry sector which involve fossil fuels burned on-site at facilities for energy. This sector also includes emissions from chemical, metallurgical, and mineral transformation processes not associated with energy consumption. CO_2 emissions ascend from land use sector primarily from deforestation, land clearing for agriculture, and fires or decay of peat soils. This estimate does not include the CO_2 that ecosystems remove from the atmosphere. The amount of CO_2 that is removed is subject to large uncertainty, although recent estimates indicate that on a global scale, ecosystems on land remove about twice as much CO_2 as is lost by deforestation [3].

So far, CO_2 emissions from agriculture mostly come from the management of agricultural soils, livestock, rice production, and biomass burning. The CO_2 emissions from transportation sector primarily involve fossil fuels burned for road,

1

rail, air, and marine transportation. Almost all (95%) of the world's transportation energy comes from petroleum-based fuels, largely gasoline and diesel. CO_2 emissions also ascend from on-site energy generation and burning fuels for heat in buildings or cooking in homes and waste water [4].
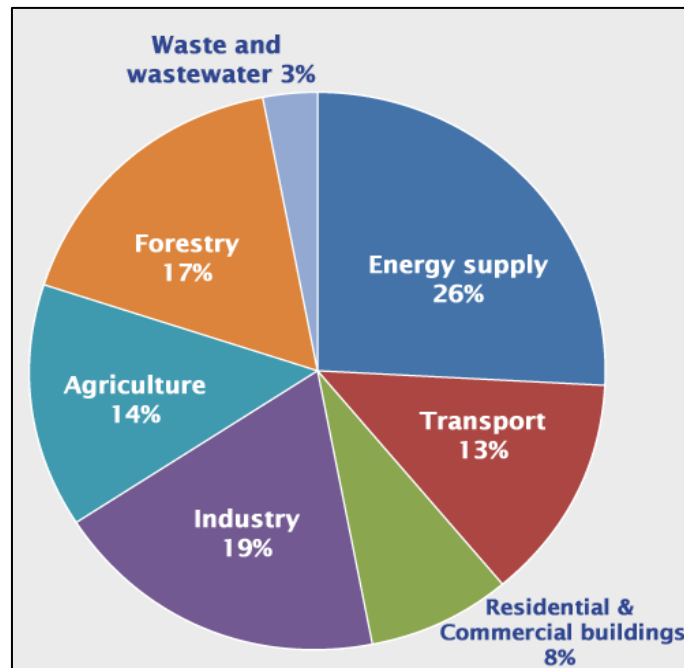
FIGURE 1.1 CO_2 Emissions by Source [2]

Global carbon emissions from fossil fuels have significantly increased since 1900. Emissions increased by over 16 times between 1900 and 2008 [4]. Therefore, CO_2 capture and sequestration from fossil-fuelled power plants is drawing increasing attention as a potential method for controlling greenhouse gas emissions. However, several technological, economic and environmental issues as well as safety problems remain to be solved, such as increasing the CO_2 capture efficiency, reducing process costs, and verifying environmental sustainability of CO_2 storage [5].

Many methods can be used for CO_2 capture such as physical absorbents by using Selexol, Rectisol; chemical absorption such as potassium carbonate, membrane separation; adsorption through zeolite and cryogenic distillation [6], organic solids, and metal-organic frameworks (MOFs). Among different developed methods, the post-combustion capture has the advantage that it can be applied to retrofit the existing power plants. The most mature technology for the CO_2 post-combustion is

the amine-based absorption due to its high affinity to CO_2 as shown in Figure 1.2 [7], [8], [9], [10], [11], [12]. However, this process belongs to the chemical separation methods which demand intensive energy use to break the chemical bonds between the absorbents and the absorbed CO_2 in the solvent regeneration step [13], [14]. Therefore, it is of benefit to find alternative solvents that compromise the high affinity for CO_2 with the ease of solvent regeneration and reuse.
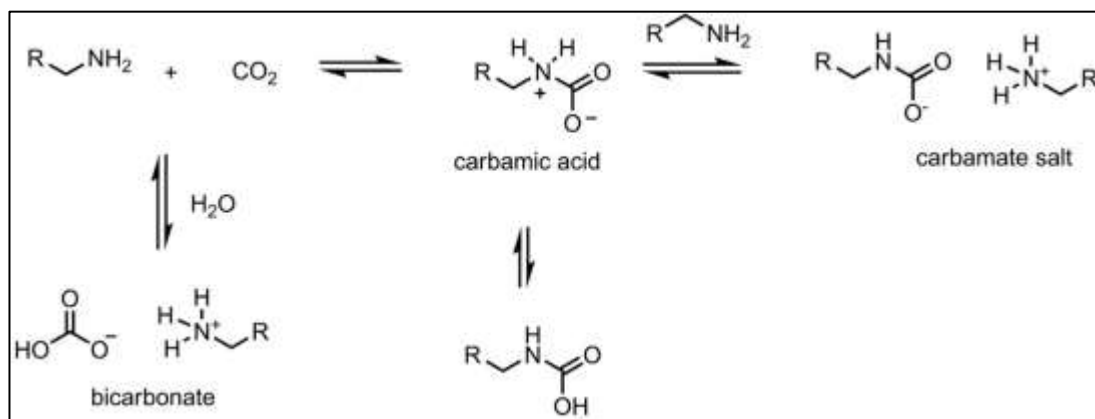
FIGURE 1.2   Amines Forming Stable Carbamates / Bicarbonates with CO_2 [10]

Green technology actively seeks new solvents to replace common organic solvents that present inherent toxicity and have high volatility, leading to evaporation of volatile organic compounds to the atmosphere. Over the past two decades, ionic liquid (ILs) has gained much attention from the scientific community, and the number of reported articles in the literature has grown exponentially. ILs is molten salts, liquid at room temperature which can be tuned by the combination of different cations and anions [15]. Nevertheless, ILs "greenness" is often challenged, mainly due to their poor biodegradability, biocompatibility, and sustainability. An alternative to ILs are deep eutectic solvents (DES), because they share many characteristics and properties with ILs such as wide liquid range, high thermal and chemical stabilities, non flammability, and high solvation capacity.

Deep eutectic solvents (DESs), known as new class of ionic liquid analogues which contain large, non-symmetric ions that have low lattice energy and hence low melting points [16]. They are usually obtained by the mixing of a substituted quaternary ammonium salts with a metal halide or a hydrogen bond donor (HBD). The charge delocalization occurring through hydrogen bonding between for example

a halide ion and the hydrogen bond donor is responsible for the decrease in the melting point of the mixture relative to the melting points of the individual components [17]. DESs are also easy to prepare in high purity thus they can be manufactured considerably lower cost than ILs [18]. Furthermore, they can be made from biodegradable components, and their toxicities are well-characterized [19].

1.2 Problem Statement

It is now well established that many ionic liquids (ILs) have the strong ability to dissolve CO_2. Similar to ILs, DESs consist predominantly of ionic species, and thus also have interesting solvent properties for high CO_2 dissolution [20]. Researchers are still trying to find new DESs which are promising and many of the research paper focusing on the DESs for CO_2 capture. Considering that combination of CO_2 with green DES systems has a great potential for a variety of chemical processes, studies on the CO_2 solubility in DESs are of prime importance [21]. However, the CO_2 absorption rate of DESs are low when compare with ILs [22].

Nowadays, DESs are more focusing on the binary mixtures between salts and HBD. A lot of new DESs are synthesized every day but most of them are not being well characterized. Density, refractive index and viscosities are among the most important characterization that requires more consideration for CO_2 capture [24].

1.3 Objectives

i.   To identify suitable combination of chemicals for a new DESs.
ii. To synthesis and identify appropriate molar ratio that will be used to form new DESs.
iii. To characterize the physical properties of DESs produced using selected tools.
iv. To measure carbon dioxide (CO_2) solubility in the DESs.

1.4   Scope of Study

This study will focuses on the synthesis and characterization of new DESs. The characterization was done by measuring the physical properties such as density, viscosity, refractive index, freezing point, and thermal stability by using thermal gravimetry analyzer of the synthesized DESs at different molar ratios and temperature. A basic study of the DESs synthesized was initiated to determine viable solvents composition. The physical properties of good DESs such as low melting point and low viscosity are being studied to improve the DESs solubility towards CO_2.

In this work, two different salts namely; potassium carbonate (K_2CO_3) and sodium acetate ($C_2H_3NaO_2$) were selected. Levulinic acid ($C_5H_8O_3$) and ethylene glycol (EG) were selected as hydrogen bond donors (HBD). Different molar ratios of DESs can be determined by using trial and error method to achieve an optimum mixing molar ratios. The resulted DESs are considered success when a colourless clear solution formed within the tolerable time setting. Several tests include thermal gravimetric analysis (TGA) test, differential scanning calorimetry (DSC) test and CO_2 absorption tests will be performed on the resulted DESs in order to determine and improve its qualities as well as its performance towards CO_2 absorption.

CHAPTER 2

LITERATURE REVIEW

The main purpose of this chapter is to attain relevant information with regards to the project from the reference books, journal and technical papers. In this chapter, the discussion will focus on the meaning of DESs and the physical properties of DESs such as density, viscosity, refractive index, and the solubility of carbon dioxide (CO_2).

2.1 Introduction to Ionic liquids (ILs) and Deep Eutectic Solvents (DESs)

Ionic liquids (ILs) have been one of the most widely studied areas in science in the past decade and are probably subject to more reviews per research paper than any other current topic [25], [26], [27]. The arbitrary definition that an ionic liquid is a class of fluids which consist of ions and are liquid at temperatures less than 100°C was used traditionally to differentiate between ionic liquids and classical molten salts, which melt at higher temperatures; however, ionic liquids are now generally referred to as solvents which consist solely of ions [28]. The ionic liquids formed from organic cations with $AlCl_3$ and $ZnCl_2$ are often termed first generation ionic liquids [25]. This class of ionic liquids are fluid at low temperatures due to the formation of bulky chloroaluminate or chlorozincate ions at eutectic compositions of the mixture. This reduces the charge density of the ions, which in turn reduces the lattice energy of the system leading to a reduction in the freezing point of the mixture.

The second generation of ionic liquids are those that are entirely composed of discrete ions such as alkylimidazolium salts which are being discovered as a stable

liquid that could be synthesized by replacing the $AlCl_3$ used in the eutectic ionic liquids with discrete anions [29]. These systems have the additional benefit of large electrochemical windows, allowing less noble metal, inaccessible from the chloroaluminate liquids to be electrodeposited [30]. However, ILs are not successful viable alternatives to current aqueous sorbent as they are neither simple nor economic to synthesize [24].

Hence, eutectic mixtures so-called deep eutectic solvents (DESs) have been recognised as low cost alternatives to ILs. They are named deep eutectic solvents because when the two constituting components are mixed together in the correct ratio, a eutectic point will occur. In fact, for instance, DESs formed from mixtures of organic halide salts with an organic compound, which is a hydrogen bond donor (HBD), are able to form hydrogen bonds with the halide ion [31]. DESs have properties comparable to ionic liquids, especially their potential as tuneable solvents that can be customised to a particular type of chemistry [32]. Generally, DESs can be described using the general formula Cat^+X^-zY where Cat^+ is in principle any ammonium, phosphonium, or sulfonium cation, and X is a Lewis base, generally a halide anion. The complex anionic species are formed between X^- and either a Lewis or Brønsted acid Y (z refers to the number of Y molecules that interact with the anion). DESs are largely classified depending on the nature of the complexing agent used, see Table 2.1.

TABLE 2.1   General Formulas for the Classification of DESs [33]

Type	General Formula	Terms
Type I	$Cat^+X^-zMCl_x$	M = Zn, Sn, Fe, Al, Ga, In
Type II	$Cat^+X^-zMCl_x$. yH2O	M = Cr, Co, Cu, Ni, Fe
Type III	Cat^+X^-zRZ	Z = $CONH_2$, COOH, OH
Type IV	$MCl_x + RZ = MCl_{x-1}^+ \cdot RZ + MCl_{x+1}^-$	M = Al, Zn and Z = $CONH_2$, OH

DESs formed from MCl_x and quaternary ammonium salts, Type I, can be considered to be of an analogous type to the well-studied metal halide or imidazolium salt systems [33]. The range of non-hydrated metal halides which have a suitably low melting point to form Type I DESs is limited; however, the scope of

deep eutectic solvents can be increased by using hydrated metal halides and choline chloride (Type II DESs). Type III DESs, formed from choline chloride and HBD, have been of interests due to their ability to solvate a wide range of transition metal species, including chlorides and oxides, see Figure 2.1 [34].

Inorganic cations generally do not form low melting point eutectics due to their high charge density; however, previous studies have shown that mixtures of metal halides with urea can form eutectics with melting points less than 150°C [35]. This work shows that a range of transition metals can be incorporated into ambient temperature eutectics, and these have now been termed Type IV DESs. It would be expected that these metal salts would not normally ionize in non aqueous media; however, $ZnCl_2$ has been shown to form eutectics with urea, acetamide, ethylene glycol, and 1,6 – hexanediol [34].
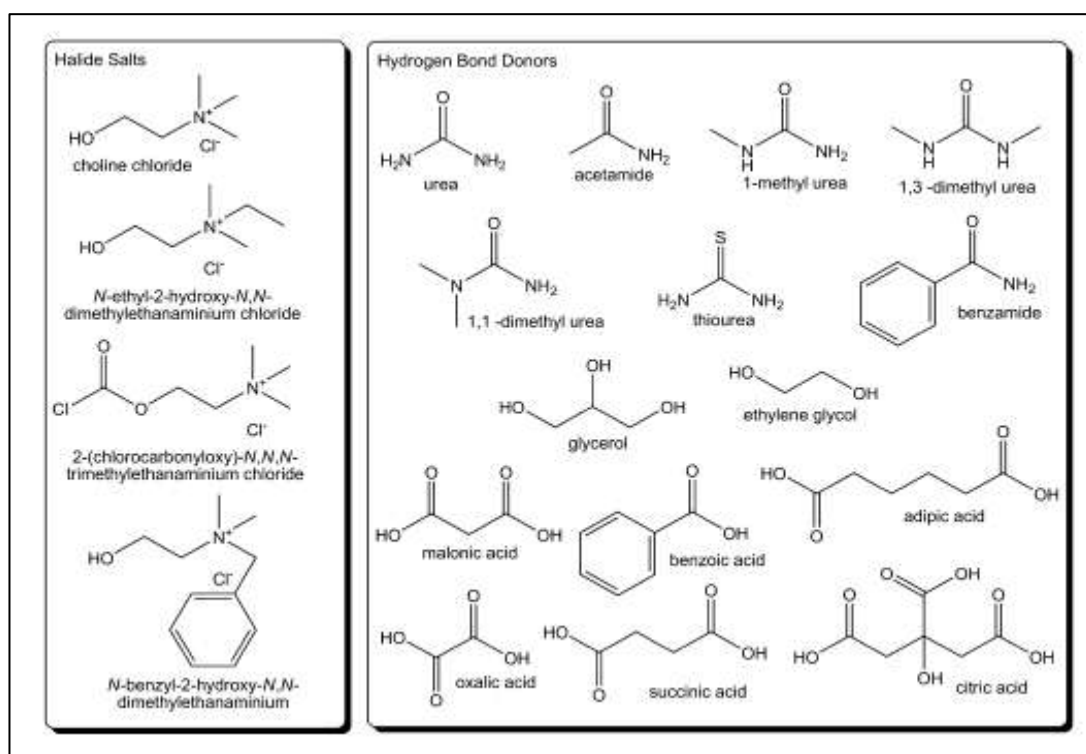
FIGURE 2.1   Structures of Some Halide Salts and Hydrogen Bond Donors used in the Formation of Deep Eutectic Solvents [34]

2.2   Physical Properties Characterization

2.2.1   Freezing/Melting Point (MP)

The difference in the melting point (ΔT_m) of deep eutectic solvents of a binary mixture consists of A and B is related to the magnitude of the interaction between A and B. The larger the interaction, the larger the ΔT_m . This is shown schematically in Figure 2.2 [36].
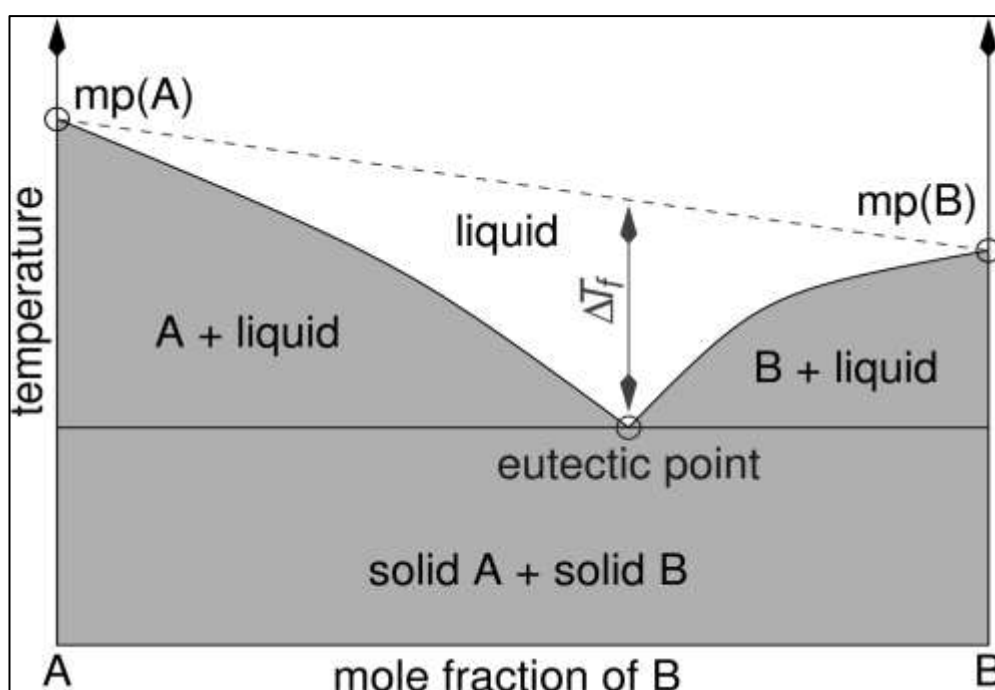
FIGURE 2.2   Schematic Representation of a Eutectic Point on a Two Component Phase Diagram [36]

In Type I eutectics, the interactions between different metal halides and the halide anion from the quaternary ammonium salt will all produce similar halometallate species with similar enthalpies of formation. This suggests that melting point (ΔT_m), values should be between 200 and 300 °C. It has been observed that to produce a eutectic at about ambient temperature the metal halide generally needs to have a melting point of approximately 300 °C or less. The same is true of the quaternary ammonium salts where it is the less symmetrical cations which have a lower melting point and therefore lead to lower melting point eutectics.

Type II eutectics are developed to include other metals into the DES formulations. It was found that metal halide hydrates have lower melting points than the corresponding anhydrous salt. Clearly the waters of hydration decrease the melting point of metal salts because they decrease the lattice energy. As Figure 2.3 shows, a lower melting point of the pure metal salt will produce a smaller depression of ΔT_f. Most of the systems studied have had phase diagrams similar to that shown in Figure 2.2, [36] except for a small number of systems containing $AlCl_3$, $FeCl_3$, and $SnCl_2$ which have each shown two eutectic points when mixed with imidazolium chlorides at approximately 33% and 66% metal halide as shown in Figure 2.4 [23].
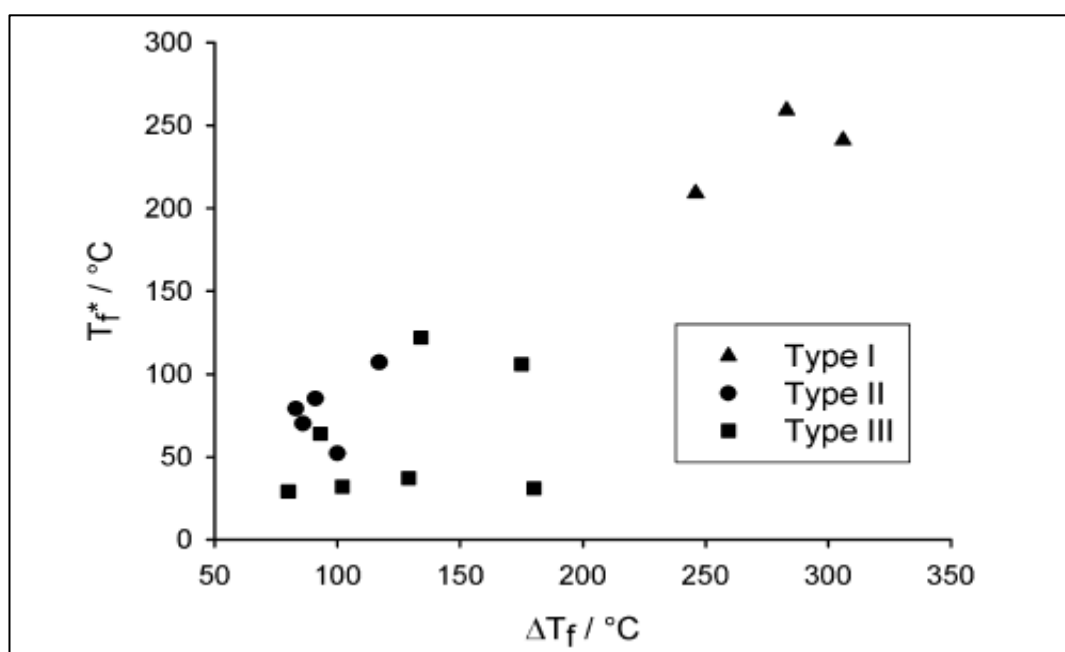
FIGURE 2.3   Correlation between the Freezing Temperature and the Depression of Freezing Point for Metal Salts and Amides when mixed with Choline Chloride in 2:1 ratio [36]

Type III eutectic mixtures depend upon the formation of hydrogen bonds between the halide anion of the salt and the HBD; where these HBDs are multifunctional, the eutectic point tends to be toward a 1:1 or 1:2 molar ratio of salt and HBD [38]. In the same study the depression of melting point was shown to be related to the mass fraction of HBD in the mixture.

TABLE 2.2   Melting Point Temperatures of a Selection of DESs [37, 38]

Halide salt	MP/ °C	HBD	MP/ °C	Salt: HBD	DESs T_m /°C
ChCl	303	Urea	134	1:2	12
ChCl	303	Thiourea	175	1:2	69
ChCl	303	1-methyl urea	93	1:2	29
ChCl	303	1,3-dimethyl urea	102	1:2	70
ChCl	303	1,1-dimethyl urea	180	1:2	149
ChCl	303	Acetamide	80	1:2	51
ChCl	303	Banzamide	129	1:2	92
ChCl	303	Adipic acid	153	1:1	85
ChCl	303	Benzoic acid	122	1:1	95
Halide salt	MP/ °C	HBD	MP/ °C	Salt: HBD	DESs T_m /°C
ChCl	303	Citric acid	149	1:1	69
ChCl	303	Malonic acid	134	1:1	10
ChCl	303	Oxalic acid	190	1:1	34
ChCl	303	Phenylacetic acid	77	1:1	25
ChCl	303	Phenylpropionic acid	48	1:1	20
ChCl	303	Succinic acid	185	1:1	71
ChCl	303	Tricarballylic acid	159	1:1	90
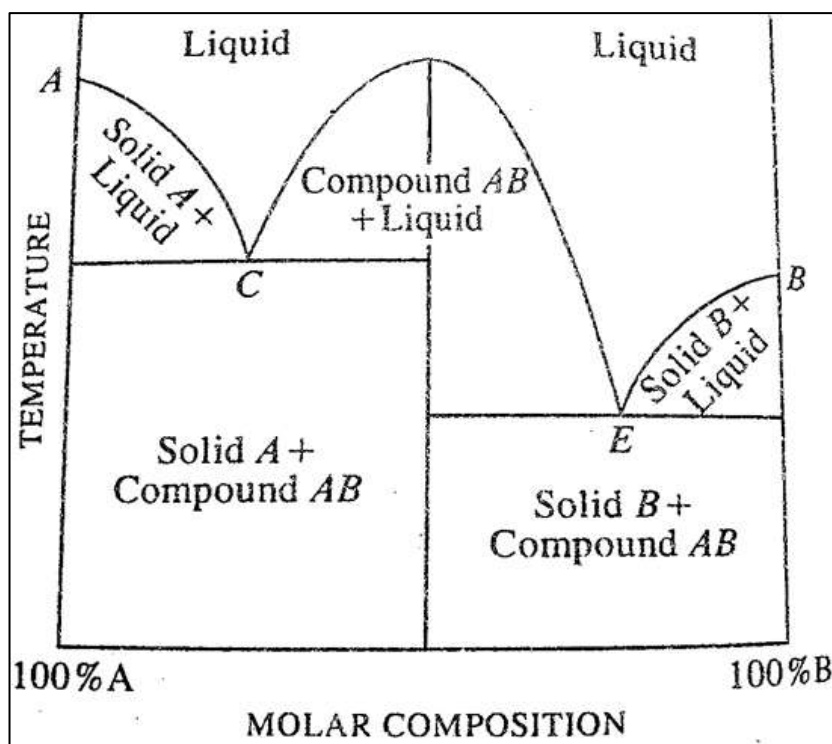
FIGURE 2.4   Schematic Representation of Exceptional Case of Two Eutectic
Points on a Two Component Phase Diagram [23]

2.2.2   Density, Viscosity and Refractive Index

Density leads to an understanding of the liquid's behaviour. It is well known
that density is drastically affected by the temperature and components of the liquid. It
is important to know the effect of temperature on density in applications such as
solvent design [39]. Density of a DES system can be predicted through the formula:

$$\rho_{DES} = \sum_{i=1}^{n} p_i X_i \tag{1}$$

where ρ is density and X_i is the mass fraction of each compounds in the DES
systems. A current study shows that density of DES increased with increasing
pressure and decreased with increasing temperature. This phenomenon can be
explained through the compressibility and expansibility of DES volumes at different
temperature and pressure [41]. The validity of equation can be improves by adding a

12

correction factor as well as a constant, forming a function either of temperature or pressure [42].

$$\rho_T = \rho_o + m_T T \qquad (2)$$

$$\rho_P = \rho_o + m_P P \qquad (3)$$

where ρ is density and m is gradient of linear fitted line using least–squares method on experimental data. Overall, density of DES is represented as a function of temperature and pressure by a Tait–type equation [41].

$$\rho(T,P) = \frac{\rho_o(T)}{1 - C\ln(B(T) + \frac{P}{B(T)} + \rho_{ref}} \qquad (4)$$

where ρ_o is the reference density; ρ_{ref} is the reference pressure (0.1 MPa); and C, B(T) are adjustable parameters determined by fitting the data into equation above by applying the Marquardt method. The parameter C is assumed to be independent of temperature while B is assumed to be temperature–dependent.
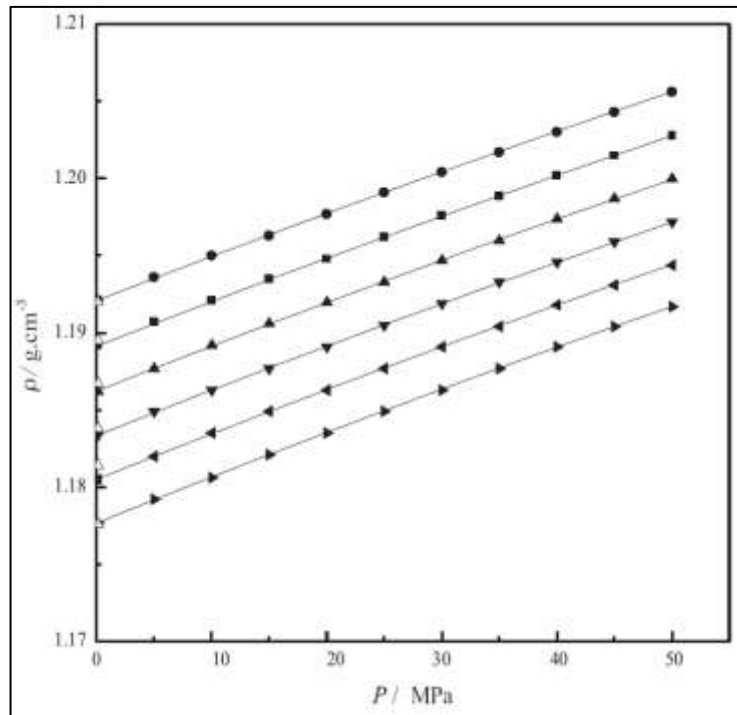
FIGURE 2.5   Density of Chcl: Gly (1:2) as a function of Pressure at Different Temperatures (298.15 K – 323.15 K) [41]

Viscosity is an internal friction measurement of a moving fluid which describes the resistance of a substance to flow [40]. In comparison to organic solvents, DESs have higher viscosity leading to some difficulties in handling, stirring and also filtering. The liquid viscosity is important in selecting an appropriate solvent. The viscosity is strongly influenced by the ability of the liquid to transport the mass within the liquid, which is immensely responsible for any changes in the chemical reactions. The high viscosity of the DES causes the limited mobility of species within the DES, which in turn causes a low conversion of products, especially in enzymatic reactions [39]. Viscosity of DES at different molar mixing ratio is found to be converged to one point as shown in Figure 2.6. Table 2.3 shows selected typical physical properties for a variety of DESs for eutectic composition at 298 K.
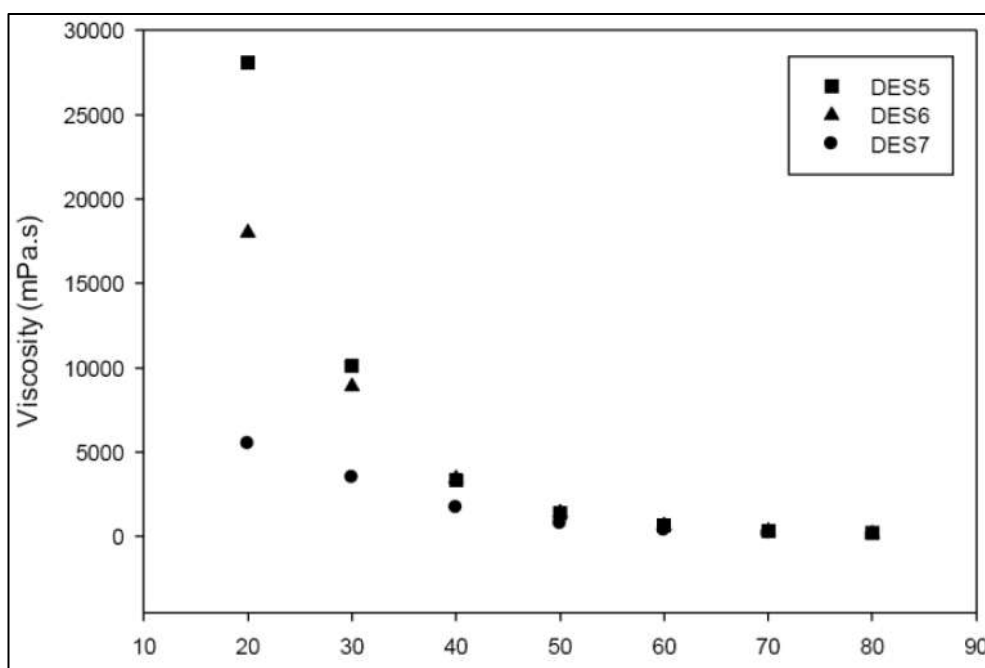
FIGURE 2.6   Dynamic Viscosity of Selected DES containing K_2CO_3 and Gly (1:4, 1:5, 1:6) as Function of Temperature [56]

TABLE 2.3   Physical Properties of DESs at 298K [18, 36]

Halide Salt	HBD	Salt:HBD	Viscosity(cP)	Density (g/cm^3)
ChCl	Urea	1:2	632	1.24
ChCl	Ethylene glycol	1:2	36	1.12
ChCl	Glycerol	1:2	376	1.18
ChCl	Malonic acid	1:1	721	-

Refractive index (RI) could be important as it might provide important information on the purity of samples and molecular interaction in the liquid. For pure DESs, RI is found to be decrease linearly with temperature. Similar with density, RI can be correlates with temperature using linear estimation of functions [42].

$$n_T = n_o + m_T T \qquad (5)$$

where n is RI and m is gradient of linear fitted line using least–squares method on experimental data. Table 2.4 shows the RI of ChCl: ethylene glycol and ChCl: glycerol DESs.

TABLE 2.4   RI of Chcl: Ethylene Glycol and Chcl: Glycerol DESs [42]

T (K)	Refractive Index	
	ChCl:Ethylene Glycol	ChCl: Glycerol
298.15	1.46823	1.48675
303.15	1.46699	1.48558
308.15	1.46575	1.48443
313.15	1.46445	1.48326
318.15	1.46320	1.48211
323.15	1.46197	1.48093
328.15	1.46078	1.47978
333.15	1.45954	1.47856

2.3 Synthesis and characterization of DESs of CO_2 capture

Despite the numerous probable applications of DESs and the advantages of their use, many of the fundamental properties of these solvents are still rather scarce in the current literature. For example, data on density, refractive index, and viscosity of DESs, which are very important physical and transport properties for any solvent system, are still limited. For this reason, the study of properties and volatility became a very important issue for any work on solvent design in this area [43]. The density is one of the important physical properties for ionic liquids in general and DESs in particular. It is also an important property for determining solvent diffusion and miscibility with other liquids [44].

It is determined the solubility of CO_2 in a choline chloride (ChCl)/urea DES at different temperatures and pressures, and for different ChCl/urea molar ratios. It has been found that the solubility of CO_2 in ChCl/urea DES depends on three factors. Firstly, the CO_2 pressure, the solubility of CO_2 increased with its pressure and was more sensitive to the pressure in the low pressure range. Secondly, the temperature, the solubility of CO_2 value decreased with an increase in the temperature whatever the pressure. Thirdly, the ChCl/urea molar ratio also has a significant effect on the solubility of CO_2 values. Similar to the case of ILs, the gaseous phase can be assumed to be pure CO_2 due to the very low vapour pressure of DESs at low temperatures (less than 60°C). Thus, Henry's constants of CO_2 in different DESs can be obtained. Choline chloride is hygroscopic and contains a small amount of water. Water acts as an anti-solvent that drives CO_2 out from the rich solutions, thereby affecting the solubility of the CO_2 [45], [46].

Earlier, [47] studied the solubility of CO_2 in ChCl/urea/H_2O DES at different temperatures (303, 308, and 313 K) and at a CO_2 pressure of 0.1 MPa. The results showed that the solubility of CO_2 in the ChCl/urea (molar ratio 1:2) DES decreased with an increase in the water content. The determination of the enthalpy of the CO_2 absorption demonstrated that ChCl/urea/H_2O is higher than 0.231 and the absorption of the CO_2 was endothermic. Below this molar ratio, the CO_2 absorption was exothermic.

The solubility of CO_2 in triethylbutyl ammonium carboxylate and water DESs at room temperature and low pressure shows that it had fast absorption rate and large absorption capacity of CO_2 [48]. Finally, it is reported that the solubilities of CO_2 increased with pressure and decreased with the increasing of the temperature in DES ChCl/ethylene glycol (molar ratio 1:2) for the temperature range of 303.15−343.15 K and pressures up to 6 MPa. The solubility data also were successfully represented by an extended Henry's law equation as a function of temperature and pressure with an average absolute deviation of 1.6%. The reported CO_2 solubility in the studied DESs was very low as compared to the amine-based absorption used in industry [45], [46].

Specifically, 17 DESs were synthesized in-house and investigated for their affinity towards CO_2, see Table 2.5. Table 2.6 also shows the summary of CO_2 solubility of DESs at different temperature and pressure.

TABLE 2.5   Experimental Solubility Values for CO_2 in DESs at 25° C and Pressure about 10 bar [49]

Components		Molar Ratio		$g_{CO_2}/g_{solvent}$
ChCl	Triethylene glycol	1	4	0.0130
ChCl	Ethylene glycol	1	4	0.0133
ChCl	Ethylene glycol	1	8	0.0168
ChCl	Urea	1	4	0.0142
ChCl	Urea	1	2.5	0.0114
ChCl	Glycerol	1	3	0.0201
ChCl	Glycerol	1	8	0.0143
ChCl	Ethanolamine	1	6	0.0749
ChCl	Ethanolamine	1	6	0.0408
Benzyltriphenylphosphonium chloride	Glycerol	1	12	0.0206
n-butyltriphenylphosphonium bromide	Ethylene glycol	1	12	0.0201
Methyltriphenylphosphonium bromide	Ethanolamine	1	6	0.0716
Methyltriphenylphosphonium bromide	Ethanolamine	1	7	0.0643
Methyltriphenylphosphonium bromide	Ethanolamine	1	8	0.0632
Tetrabutylammonium bromide	Ethanolamine	1	6	0.0591
Tetrabutylammonium bromide	Diethanolamine	1	6	0.0373
Tetrabutylammonium bromide	Triethanolamine	1	3	0.0207

TABLE 2.6 CO$_2$ Solubilities in ChCl-Urea DESs System at Different Temperature and Pressure [50]

T (K)	P (MPa)	Molar Ratio		CO$_2$ Solubility (mol/kg)
		ChCl	Urea	
303.15	0.299	1	2	0.2784
	0.813	1	2	0.7342
	1.993	1	2	1.6355
	2.763	1	2	2.1591
	4.104	1	2	2.8635
	5.654	1	2	3.5592
313.15	0.350	1	2	0.2694
	0.818	1	2	0.5949
	2.021	1	2	1.3927
	2.795	1	2	1.8339
	4.144	1	2	2.5200
	4.616	1	2	2.6421
	5.722	1	2	3.1151
323.15	0.356	1	2	0.2269
	0.825	1	2	0.5083
	2.044	1	2	1.1929
	2.838	1	2	1.5721
	4.108	1	2	2.1650
	4.709	1	2	2.3745
	5.728	1	2	2.7870
333.15	0.362	1	2	0.1923
	0.832	1	2	0.4371
	2.061	1	2	0.9909
	2.874	1	2	1.3476
	4.251	1	2	1.8766
	4.918	1	2	2.0987
	5.845	1	2	2.3945

2.4   Material Selection

The synthesised DESs were chosen based on the structure of salt and the HBD. Materials selected for this project are potassium carbonate, sodium acetate as salt, levulinic acid and ethylene glycol as HBD.

2.4.1   Potassium Carbonate (K_2CO_3)
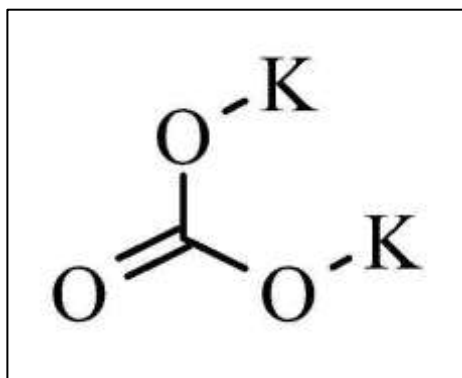
FIGURE 2.7   IUPAC Structure of Potassium Carbonate [52]

TABLE 2.7   Properties of Potassium Carbonate [52]

Physical State	Solid
Odour	Odourless
Molecular Weight	138.21 g/mole
Colour	White
Boiling Point	Decomposes
Specific Gravity	2.29
Solubility	Soluble in cold water

2.4.2 Sodium Acetate ($C_2H_3NaO_2$)
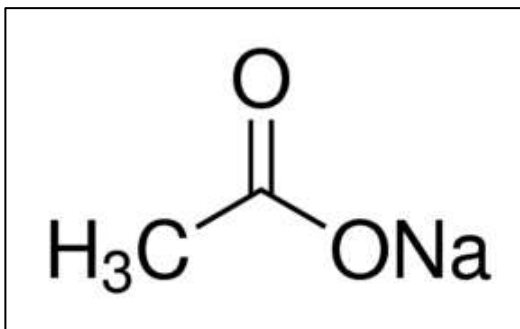
FIGURE 2.8   IUPAC Structure of Sodium Acetate [53]

TABLE 2.8   Properties of Sodium Acetate [53]

Physical State	Solid
Odour	Slightly odourless to acetic
Molecular Weight	82.03 g/mole
Colour	White
Melting Point	324°C
Specific Gravity	1.528
Solubility	Easily soluble in cold water and hot water

2.4.3 Levulinic Acid ($C_5H_8O_3$)
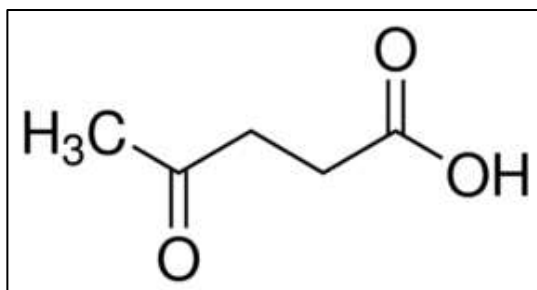
FIGURE 2.9   IUPAC Structure of Levulinic Acid [54]

TABLE 2.9　　　Properties of Levulinic Acid [54]

Physical State	Solid
Molecular Weight	116.12 g/mole
Boling Point	245.5°C
Melting Point	34°C
Specific Gravity	1.1447

2.4.4　Ethylene Glycol
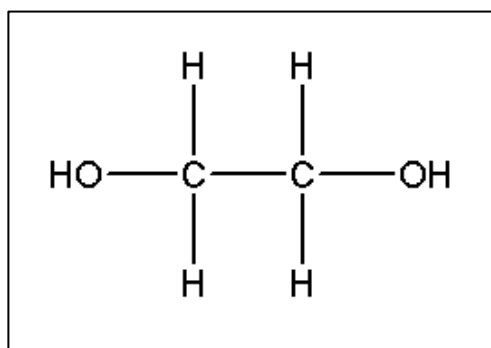
FIGURE 2.10　　　IUPAC Structure of Ethylene Glycol [55]

TABLE 2.10　　　Properties of Ethylene Glycol [55]

Physical State	Liquid
Odour	Odourless
Molecular Weight	62.07 g/mole
Colour	Colourless
Boling Point	197°C
Melting Point	-12°C
Specific Gravity	1.113
Solubility	Miscible

CHAPTER 3

METHODOLOGY

3.1   Materials and Apparatus

Potassium carbonate (K_2CO_3), sodium acetate ($C_2H_3NaO_2$), levulinic acid ($C_5H_8O_3$), and ethylene glycol (EG) are purchased from Merck Chemicals as well as Sigma-Aldrich Chemicals. The equipments related to the project are as in Table 3.1.

TABLE 3.1   Equipment List for the Project

Equipment	Brand	Function	Location
Hot Magnetic Stirring Plate	-	Heating and mixing	Block 05-01-05
Vacuum Oven	Memmert	Moisture removal from DESs	Block 03-02-03

Thermal Gravimetry Analyzer	Perkin Elmer STA6000	Evaluate the thermal stability of DESs	Block 04-01-06
Differential Scanning Calorimetry	Mettler Toledo DSC1	Evaluate the melting point of DESs	Block 04-01-06
Density Meter	Anton Paar	Observe the changes of density at different temperature	Block 04-01-06
Viscometer	Anton Paar LOVIS 2000M	Determine the viscosity of DESs at different temperature	Block 04-01-06

Refractometer	Atago RX-5000α	Study the changes of refractive index at different temperature.	Block 03-00-06
High Pressure Gas Solubility Cell	Solteq	Gas absorption/release experiment.	Block 03-00-06

3.2 Methodology

In this research, new DESs will be synthesized and characterized, and the solubility of CO_2 will be studied. The prepared DESs are chosen based on the structure of salts and the HBD.

3.2.1 Synthesis of DESs System

In order to prepare DESs mixtures, a binary DES mixture of K_2CO_3 and levulinic acid is first prepared by mixing both of them in the appropriate molar ratio under vigorous stirring at 80°C until the resulting solutions are clear and homogeneous. The solution is left overnight at room temperature to ensure no precipitation happened. After that, the solvent is dried at 70°C under 200 mBar in the vacuum oven for 48 hours. At this point, the DESs are ready for use. It is important to note that no purification step is required and no additional solvents are employed in the preparation of these DESs.

3.2.2 Characterization of DESs

The DES will be characterized by studying physicochemical properties such as density, viscosity, refractive index, decomposition temperature, and freezing point by using thermal gravimetric analysis (TGA) test and differential scanning calorimeter (DSC) test over temperature range of 298.15 K up to 328.15 K at atmospheric pressure for the whole range of composition.

3.2.3 CO_2 Capture and Release Experiment

The SOLTEQ High Pressure Gas Solubility Cell (Model: BP-22) will be used for the gas solubility measurement. The solubility of CO_2 in DESs will be measured in different molar ratio over the pressure range of 5 bar to 20 bar and temperature at 303.15 K.

3.3 Relevancy and Feasibility of the Project

This project is relevant to be completed using equipment available in the lab provided by Universiti Teknologi Petronas (UTP). Based on the timeline of the project, this project is allocated five months to be completed. All the physical properties and parameters related are being chosen wisely so that there will be enough time to complete the objectives stated. On top of that, comprehensive planning has been developed for each part of the project so that it will give an excellent result. This project also will contribute to the research on new DESs using different salt and HBD selected.

3.4 Gantt Chart and Key Milestones

The gantt chart is as Table 3.2, and key milestones are starred.

TABLE 3.2   Gantt Chart with Key Milestones

Task / Week	FYP I 1	2	3	4	5	6	7	8	9	10	11	12	13	14	FYP II 1	2	3	4	5	6	7	8	9	10	11	12	13	14
Introduction to FYP / Meeting with Supervisor	■	★																										
Literature Review / Finding chemical / Preparing the methodology		■	■	■	■	■	■	■	■	■	■																	
Procurement of Lab Space, Equipment, and Chemicals Submission of Extended Proposal		■	■	■	■	■	■	★	■	■	■																	
Proposal Defence									★																			
Synthesis of DESs											■	■	■		■	■	■	■	■	■	■							
Submission of Interim Report												■	★															
Submission of Progress Report																			■	■	★							
Characterization of DESs												■	■		■	■	■	■	■	■	■	■	■	■	■	■	■	■
Submission of Draft Final Report																								■	■	★		
Submission of Dissertation																										■	★	
Submission of Technical Paper																										■	★	
Viva																											■	■
Submission of Project Dissertation																												★

27

CHAPTER 4

RESULT AND DISCUSSION

4.1   Formation of Solvents

In this study, two different salts namely; potassium carbonate (K_2CO_3) and sodium acetate ($C_2H_3NaO_2$) were selected. Levulinic acid ($C_5H_8O_3$) and ethylene glycol (EG) were selected as hydrogen bond donors (HBD). Different molar ratios of DESs are determined by using trial and error method to achieve an optimum mixing molar ratios. 19 samples of DESs are prepared as described in Table 4.1. Different samples of DESs were prepared by varying the molar ratio of levulinic acid and ethylene glycol and fixed the amount of salt.

TABLE 4.1   Compositions and Abbreviations for the studied DESs

Molar Ratio	Abbreviation	Appearance at room temperature
1 K_2CO_3 : 2 Levulinic Acid	DES 1	Yellow semisolid
1 K_2CO_3 : 3 Levulinic Acid	DES 2	Yellow semisolid
1 K_2CO_3 : 4 Levulinic Acid	DES 3	Yellow semisolid
1 K_2CO_3 : 5 Levulinic Acid	DES 4	Yellow semisolid
1 K_2CO_3 : 6 Levulinic Acid	DES 5	Yellow semisolid
1 K_2CO_3 : 7 Levulinic Acid	DES 6	Yellowish clear solution
1 K_2CO_3 : 8 Levulinic Acid	DES 7	Yellowish clear solution
1 K_2CO_3 : 9 Levulinic Acid	DES 8	Yellowish clear solution
1 K_2CO_3 : 2 Ethylene Glycol	DES 9	White semisolid
1 K_2CO_3 : 3 Ethylene Glycol	DES 10	White semisolid
1 K_2CO_3 : 4 Ethylene Glycol	DES 11	Turbid white liquid
1 Sodium Acetate : 2 Levulinic Acid	DES 12	Yellowish clear solution
1 Sodium Acetate : 3 Levulinic Acid	DES 13	Yellowish clear solution
1 Sodium Acetate : 4 Levulinic Acid	DES 14	Yellowish clear solution
1 Sodium Acetate : 2 Ethylene Glycol	DES 15	White semisolid
1 Sodium Acetate : 3 Ethylene Glycol	DES 16	White semisolid
1 Sodium Acetate : 4 Ethylene Glycol	DES 17	Colourless liquid
1 Sodium Acetate : 5 Ethylene Glycol	DES 18	Colourless liquid
1 Sodium Acetate : 6 Ethylene Glycol	DES 19	Colourless liquid

From Table 4.2, it can be clearly seen that sodium acetate and levulinic acid form eutectics at a ratio of 1:2, 1:3, and 1:4. The criteria of selecting feasible eutectic solvents includes, the solvent is clear at the end of mixing, liquid phase at room temperature (20°C), less than 120 minutes of mixing time at 80°C under 400 rpm of stirring and no recrystallization of solids happened after the resultant solvent is sealed with parafilm and left untouched for 24 hours.

TABLE 4.2   Eutectic Solvents formed with Sodium Acetate and Levulinic Acid at different ratio

Sodium Acetate : Levulinic Acid
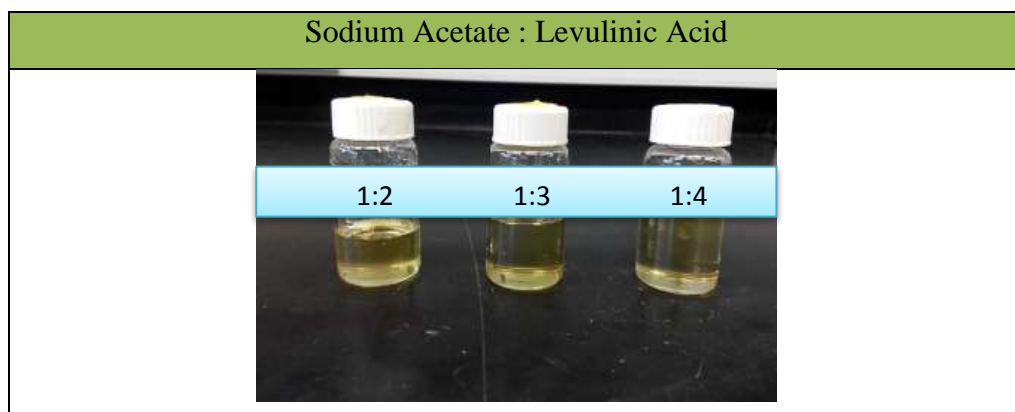
Table 4.3 shows that sodium acetate with ethylene glycol form colourless liquid at a ratio of 1:4, 1:5, and 1:6. For molar ratio of 1:2 and 1:3, the solvents form recrystallization of solids during the mixing time under 400 rpm of stirring and were not successful. The existence of solid particles in the mixture indicates that the amount of salt is in excess to the corresponding HBD which results in the precipitation of the extra amount of salt which cannot build hydrogen bonds with the HBD. Adding more ethylene glycol (as in DES 17, DES 18 and DES 19) achieved the required stability between the two DES constituents and ensures complete dissolution and formed a colourless liquid phase.

TABLE 4.3   Eutectic Solvents formed with Sodium Acetate and Ethylene Glycol at different ratio

Sodium Acetate : Ethylene Glycol
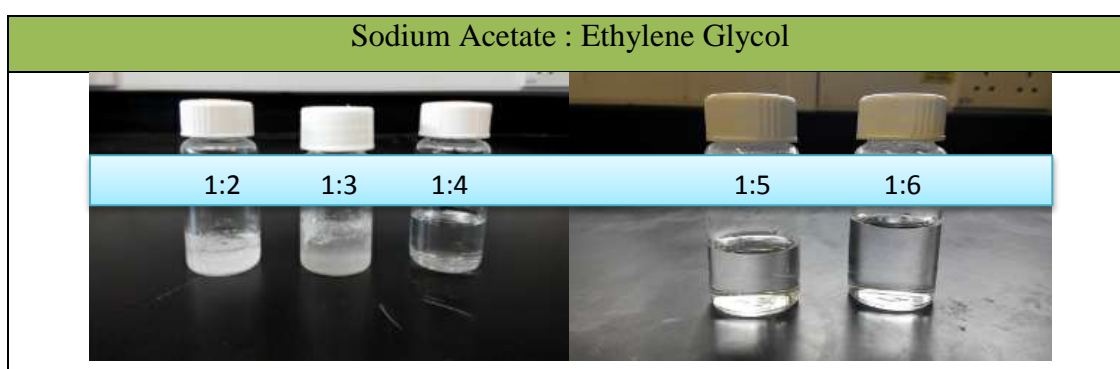
A similar synthesis procedure was used for the potassium carbonate based salt. Low salt to HBD molar ratios (DES 1, DES 2, DES 3, DES 4 and DES 5) were not successful and hence were removed from further analysis. Molar ratios starting from

1:7 to 1:9 (DES 6, DES 7 and DES 8) were successful and appeared as yellowish clear solutions. From Table 4.4, it can be seen that potassium carbonate with levulinic acid form eutectics at a ratio of 1:7, 1:8, and 1:9. For molar ratio of 1:2, 1:3, and 1:4, the solvents form recrystallization of solids during the mixing time. As for 1:5 and 1:6 molar ratio of the solvent, the solutions form crystal solid after being allowed to cool at room temperature.

TABLE 4.4   Eutectic Solvents formed with Potassium Carbonate and Levulinic Acid at different ratio

Potassium Carbonate : Levulinic Acid

| 1:2 | 1:3 | 1:4 | 1:5 | 1:6 | 1:7 | 1:8 | 1:9 |
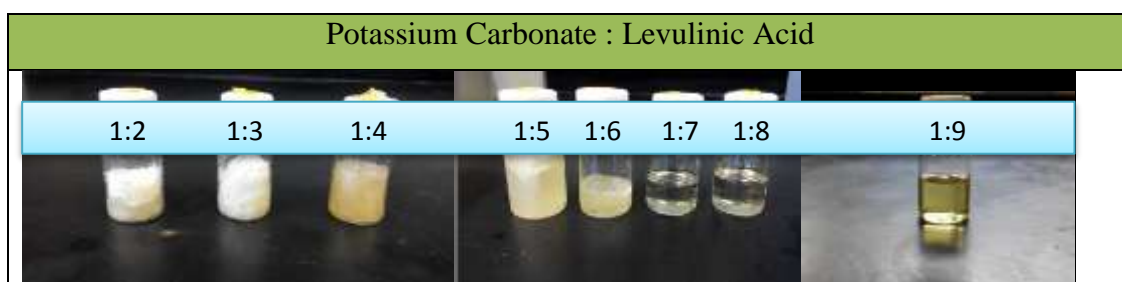
In Table 4.5, it shows that potassium carbonate and ethylene glycol form a solution with precipitation at a ratio of 1:2, 1:3, and 1:4 after it being allowed to cool at room temperature for 24 hours. The three unsuccessful DESs (DES 9, DES 10 and DES 11) were not studied further.

TABLE 4.5   Solvents formed with Potassium Carbonate and Ethylene Glycol at different ratio

Potassium Carbonate : Ethylene Glycol

| 1:2 | 1:3 | 1:4 |
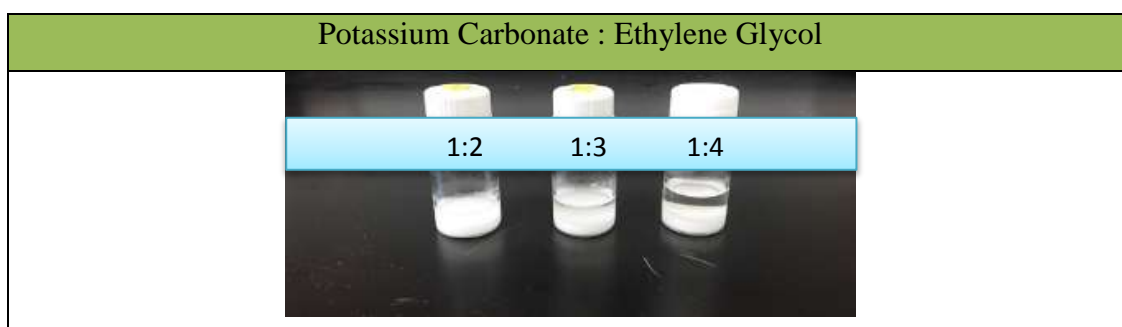
From all the binary mixtures, it can be deduced that levulinic acid and ethylene glycol as HBD can perform well with sodium acetate as well as potassium carbonate as salt. Although ethylene glycol does not form eutectics with potassium carbonate with a ratio of 1:2, 1:3 and 1:4, it had been discovered based on the recent study that

ethylene glycol can form eutectics with potassium carbonate with ratio of 1:6, 1:7, and 1:8 [57].

For the characterization process, potassium carbonate, sodium acetate with different HBD consists of different ratios of levulinic acid and ethylene glycol is mixed as in Table 4.6.

TABLE 4.6   Mass of Individual Component of the studied DESs

	DES 1		DES 2		DES 3		DES 4		DES 5		DES 6	
	Salt	HBD	Salt	HBD	Salt	HBD	Salt	HBD	Salt	HBD	Salt	HBD
Mass (g)	4.1464	6.9672	4.1463	10.4510	4.1464	13.9342	4.1465	17.4180	4.1464	20.9015	4.1464	24.3852
Mol	0.0300	0.0600	0.0300	0.0900	0.0300	0.1199	0.0300	0.1500	0.0300	0.1799	0.0300	0.2100
Molar ratio	1	2	1	3	1	4	1	5	1	6	1	7

	DES 7		DES 8		DES 9		DES 10		DES 11		DES 12	
	Salt	HBD	Salt	HBD	Salt	HBD	Salt	HBD	Salt	HBD	Salt	HBD
Mass (g)	4.1464	27.8689	4.1463	31.3524	4.1465	3.7244	4.1466	5.5864	4.1464	7.4483	2.4612	6.9670
Mol	0.0300	0.2400	0.0300	0.2700	0.0300	0.0600	0.0300	0.0900	0.0300	0.1199	0.0300	0.0599
Molar ratio	1	8	1	9	1	2	1	3	1	4	1	2

	DES 13		DES 14		DES 15		DES 16		DES 17		DES 18	
	Salt	HBD	Salt	HBD	Salt	HBD	Salt	HBD	Salt	HBD	Salt	HBD
Mass (g)	2.4611	10.4510	2.4611	13.9342	2.4610	3.7244	2.4610	5.5868	2.4610	7.4485	2.4609	9.3107
Mol	0.0300	0.0900	0.0300	0.1199	0.0300	0.0600	0.0300	0.0900	0.0300	0.1200	0.0300	0.1500
Molar ratio	1	3	1	4	1	2	1	3	1	4	1	5

	DES 19	
	Salt	HBD
Mass (g)	2.4610	11.1726
Mol	0.0300	0.1800
Molar ratio	1	6

4.2   Thermal Analysis

4.2.1   Decomposition Temperature

The range in which the prepared DESs are stable and are liquid, was evaluated using thermal gravimetric analysis (TGA) is conducted by means of determining the decomposition temperature. Thermal gravimetric analysis is a method where a sample is measured as a function of time and temperature while the sample is subjected to a linear temperature program or an isotherm in a controlled atmosphere. The precision of TGA result in measuring the decomposition temperature can be influenced by various basic parameters and condition, such as temperature, pressure, molar ratio of sample, and heating rate.

The DESs samples are heated up from 323.15 K to 773.15 K at a scanning rate of 5K/min. To avoid oxidation, all DESs samples are put under continuous nitrogen flow of 20mL/min. From the dynamic scan data, the decomposition temperature is derived. This temperature is determined as the temperature at the intersection of extrapolated constant mass and the slope of the mass loss at inflection point. The result shows is significantly reliant on the scanning rate where the lower the ramp, the resolution will increase. Besides, higher heating rate may effect in small changes in TGA curve, displaying a higher decomposition temperature than the actual point at which the DESs is thermally stable [58, 59]. Results are presented in Table 4.7 and in Figure 4.1.

In Table 4.7, it can be seen that the decomposition temperature of DESs increased when more HBD is added into the system. Similar trend is observed in DES 12, DES 13, DES 14, DES 17, DES 18 and DES 19. Among all the DESs samples, DES 6 (1 K_2CO_3:7 Levulinic Acid) is having the highest thermal stability and decomposition temperature. Overall, as HBD content in DESs increased, the thermal stability of DESs is increased.

Although similar trend is observed in the DESs system, there are some exemptions. For DES 6, DES 7 and DES 8, as levulinic acid content in the DESs increased, decomposition temperature of DESs decrease. This may be due to addition of levulinic acid is disrupting the saturated strong hydrogen bonding between potassium carbonate with levulinic acid.
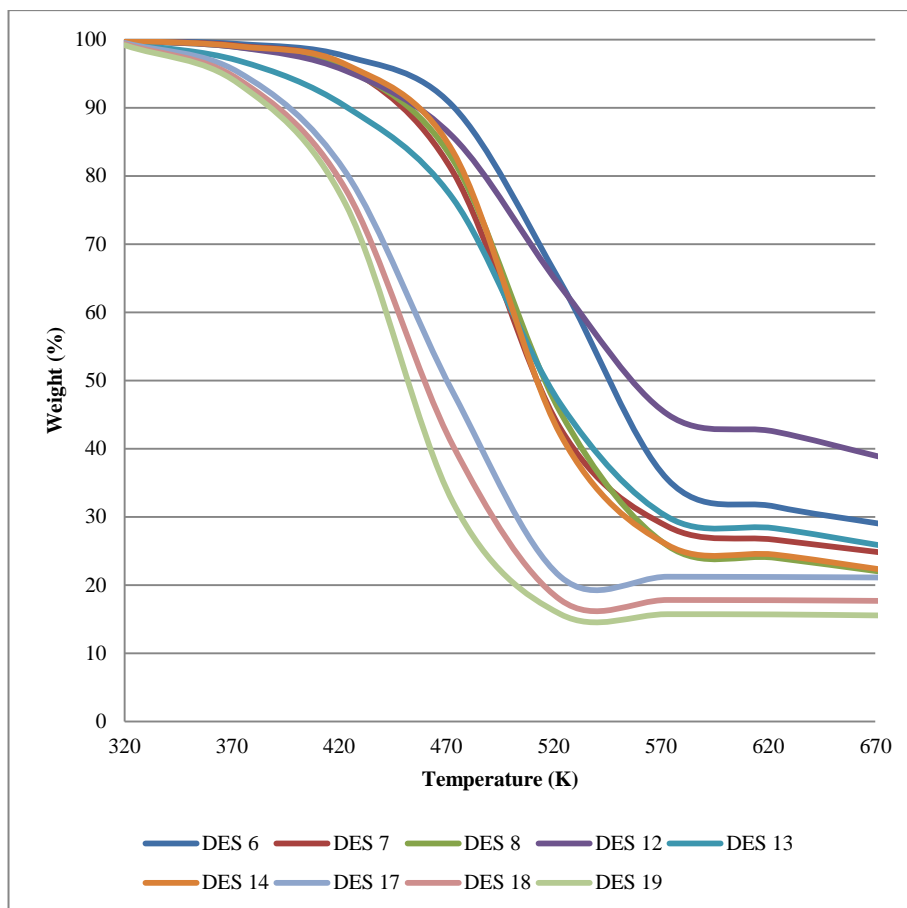
FIGURE 4.1   TGA Curves of DESs

TABLE 4.7   Decomposition Temperature Data of DESs

Abbreviations	Molar Ratio	$T_{decomposition}$ (K)
DES 6	1:7	457.81
DES 7	1:8	447.09
DES 8	1:9	444.00
DES 12	1:2	425.86
DES 13	1:3	434.82
DES 14	1:4	436.48
DES 17	1:4	394.88
DES 18	1:5	396.65
DES 19	1:6	404.45

4.2.2 Freezing Point / Glass Transition Temperature (T_g)

The freezing/melting point of DESs is the most significant in defining their liquidity range. Differential scanning calorimetry (DSC) is conducted on all DES samples to determine the freezing/melting point. The accuracy of DSC result in determining the freezing/melting point of DESs can be influenced by various parameters and condition, such as temperature, pressure, molar ratio, heating rate, and moisture content. Freezing/melting point is determined based on changes of amount of heat needed to increase the temperature of a sample which are measured as a function of temperature.

The DESs samples are first cooled to 223.15 K and heated up to 223.15 K again to 373.15 K at a scanning rate of 10K/min under continuous nitrogen flow of 20mL/min to avoid oxidation of samples. The DESs samples are then it is cooled down to 223.15K at a scanning rate of 10K/min under continuous nitrogen flow of 20mL/min, before reheat it up to 373.15K again under the same conditions. The resolution of result is highly dependant on the scanning rate where the lower the ramp, the higher the resolution. The melting point of DESs is studied at the intersection of extrapolated constant mass and the slope of the mass loss at inflection point. Results are presented in Table 4.8.

From the result as shown in Table 4.8, some DESs do not show their freezing point but rather a glass transition with enthalpy relaxation is observed. Therefore, the resultant solvents are categorized under the term 'low transition temperature mixtures' (LTTM) rather than DESs. LTTMs are attractive as solvents, since they display similar properties as imidazolium-based ILs so it can be advantageous to replace them [62], many ILs have a strong ability to dissolve CO_2 [63]. Similar to ILs, LTTMs consist mainly of ionic species and thus have remarkable solvent properties for high CO_2 solubility [62].

TABLE 4.8   Freezing Point (T_f) / Glass Transition Temperature (T_g)

Molar Ratio	Abbreviations	T_f (°C)	T_g (°C)
Pure Ethylene Glycol	-	-12	-
Pure Levulinic Acid	-	34	-
Pure K_2CO_3	-	899	-
Pure Sodium Acetate	-	324	-
1 K_2CO_3 : 7 Levulinic Acid	DES 6	59	-
1 K_2CO_3 : 8 Levulinic Acid	DES 7	48	-
1 K_2CO_3 : 9 Levulinic Acid	DES 8	-	-53
1 Sodium Acetate : 2 Levulinic Acid	DES 12	-	-38
1 Sodium Acetate : 3 Levulinic Acid	DES 13	-	-49
1 Sodium Acetate : 4 Levulinic Acid	DES 14	-	-52
1 Sodium Acetate : 4 Ethylene Glycol	DES 17	6	-
1 Sodium Acetate : 5 Ethylene Glycol	DES 18	2	-
1 Sodium Acetate : 6 Ethylene Glycol	DES 19	-	-92

4.3   Physical Properties

4.3.1   Density

Density is an important property for determining solvent diffusion and miscibility with other liquids. The densities of all synthesized DESs at all salt/HBD ratios were measured at different temperatures that ranges from 293.15 K to 353.15 K. The densities of all DESs sample are measured as a function of temperature and are depicted in Figure 4.2 and Table 4.9 to 4.11. The effect of temperature on DES density was explored. From the observation in Figure 4.2, the density decreased linearly with increasing temperature. The decreases in density with respect to temperature are the results of volume increase due to thermal expansion and gains in both vibrational and translational energy of the DES ensembles and free ions [51]. These vibrations can cause molecular rearrangements due to the weak interactions between ions, which in turn decreases the density of the liquid [60]. The density of

DES decreased with increasing molar ratio of HBD in all DESs samples. The dotted lines in Figure 4.2 show that density of DESs can be fitted with linear fit in the form of Equation 6.

$$\rho = mT + c \qquad (6)$$

where ρ is density of DESs, T is temperature in Kelvin while m and c are the fitting parameters varied for different DESs. Table 4.12 shows the fitting parameters of density of each DES.

TABLE 4.9   Density versus Temperature Data for DES 8 over the temperature range (293.15 - 353.15) K

T/K	Density (DES 8) (g/cm^3)
293.15	1.2174
303.15	1.2090
313.15	1.2004
323.15	1.1924
333.15	1.1842
343.15	1.1763
353.15	1.1684

TABLE 4.10   Density versus Temperature Data for DES (12, 13 and 14) over the temperature range (293.15-353.15) K

T/K	Density (DES 12) (g/cm^3)	Density (DES 13) (g/cm^3)	Density (DES 14) (g/cm^3)
293.15	1.2318	1.2091	1.1950
303.15	1.2232	1.2003	1.1864
313.15	1.2144	1.1917	1.1780
323.15	1.2058	1.1834	1.1697
333.15	1.1974	1.1751	1.1614
343.15	1.1891	1.1668	1.1531
353.15	1.1809	1.1586	1.1449

TABLE 4.11   Density versus Temperature Data for DES (17, 18 and 19) over the temperature range (293.15-353.15) K

T/K	Density (DES 17) (g/cm^3)	Density (DES 18) (g/cm^3)	Density (DES 19) (g/cm^3)
293.15	1.1999	1.1864	1.1763
303.15	1.1927	1.1794	1.1693
313.15	1.1858	1.1725	1.1625
323.15	1.1789	1.1656	1.1555
333.15	1.1721	1.1586	1.1486
343.15	1.1651	1.1517	1.1417
353.15	1.1582	1.1448	1.1347

TABLE 4.12   Result of Regression Analysis of Density versus Temperature Data for DES over the temperature range (293.15-353.15) K

Abbreviations	m	c	R^2
DES 8	-0.0008	1.4564	0.9998
DES 12	-0.0008	1.4806	0.9998
DES 13	-0.0008	1.4549	0.9999
DES 14	-0.0008	1.4393	1.0000
DES 17	-0.0007	1.4029	1.0000
DES 18	-0.0007	1.3896	1.0000
DES 19	-0.0007	1.3793	1.0000
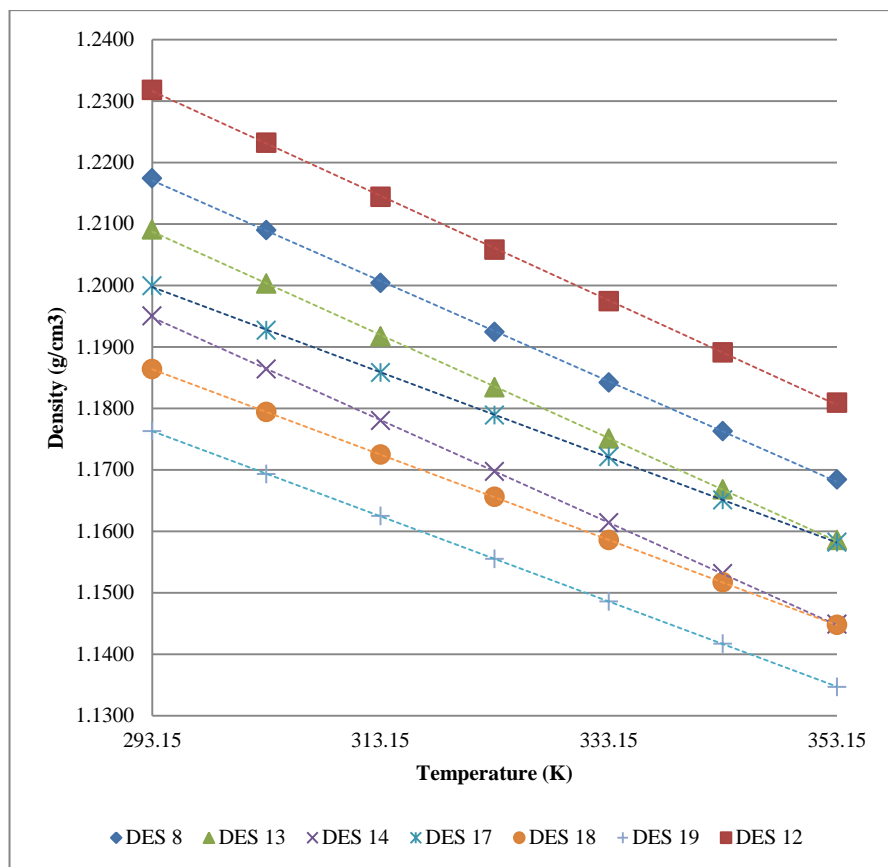
FIGURE 4.2   Density of DES against temperature range (293.15-353.15) K

4.3.2   Viscosity

The viscosity of DESs is highly influenced by the selection of the HBD and salt driven by their structures that determine the nature of intermolecular interactions between the molecules and ions in solution. Viscosity is a measure of resistance of fluid against shear or tensile stress and expression of strength of the molecular interactions within components of a fluid. It is a crucial property because it strongly influences the rate of mass transport in the solvent. The viscosities of DESs have been measured as a function of temperature and are displayed in Figure 4.3 and Table 4.13 to 4.15. All the DESs samples show that the viscosity values reduce as the temperature increases from 293.15 K to 353.15 K. This happened because of the mobility of ions. The massive difference in densities indicates that the DESs are highly sensitive towards temperature. Increased kinetic energy through heating may weaken the attractive forces between molecules [60].
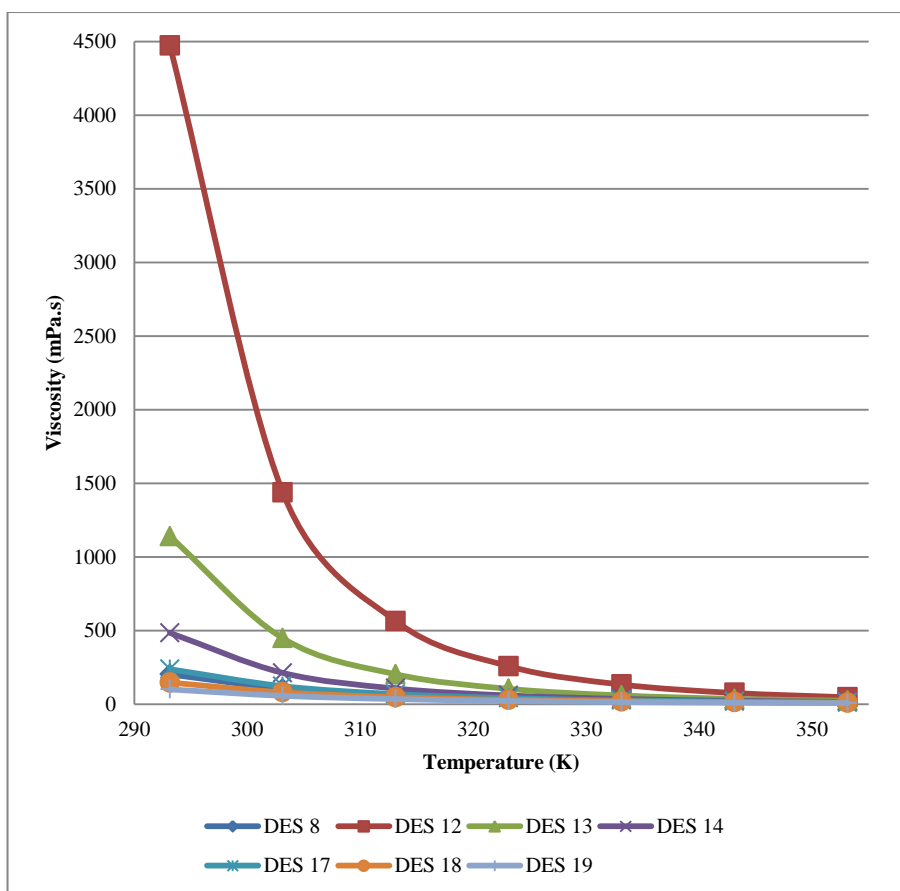
FIGURE 4.3   Viscosity of DES against temperature range (293.15-353.15) K

TABLE 4.13   Viscosity versus Temperature Data for DES 8 over the temperature range (293.15-353.15) K

T/K	Viscosity (DES 8) (mPa.s)
293.15	203.49
303.15	106.49
313.15	61.006
323.15	39.479
333.15	26.923
343.15	19.252
353.15	14.278

TABLE 4.14   Viscosity versus Temperature Data for DES (12, 13 and 14) over the temperature range (293.15-353.15) K

T/K	Viscosity (DES 12) (mPa.s)	Viscosity (DES 13) (mPa.s)	Viscosity (DES 14) (mPa.s)
293.15	4472.8	1140.3	485.40
303.15	1437.9	448.99	213.79
313.15	565.55	204.31	107.56
323.15	259.00	105.59	60.346
333.15	134.61	60.466	36.955
343.15	77.319	37.607	24.288
353.15	48.099	24.987	16.808

TABLE 4.15   Viscosity versus Temperature Data for DES (17, 18 and 19) over the temperature range (293.15-353.15) K

T/K	Viscosity (DES 17) (mPa.s)	Viscosity (DES 18) (mPa.s)	Viscosity (DES 19) (mPa.s)
293.15	238.72	148.38	101.56
303.15	123.47	81.578	58.182
313.15	69.664	48.387	35.779
323.15	42.390	30.597	23.213
333.15	27.508	20.482	15.915
343.15	18.819	14.372	11.382
353.15	13.449	10.487	8.441

The dependence of viscosity towards temperature can be described through Vogel-Tamman-Fulcher (VTF) equation below:

$$\ln(\eta) = a + \frac{b}{T - c} \qquad (7)$$

where η (mPa.s) is the dynamic viscosity, T is the temperature in Kelvin while a, b, and c are fitting parameters as in Table 4.16. The fitting parameters are determined based on graph plotting of ln η versus 1/T as in Figure 4.4.

TABLE 4.16   Result of Regression Analysis of ln η versus 1/T according to equation for DES over the temperature range (293.15-353.15) K

DES	a	b	c	R^2
DES 8	-6.53547	2460.64117	85.52	0.9879
DES 12	-7.27369	2313.66111	145.59	0.9858
DES 13	-7.62158	2495.67847	122.92	0.9874
DES 14	-7.55280	2542.72418	108.06	0.9881
DES 17	-6.99845	2497.19332	92.954	0.9925
DES 18	-6.81338	2451.27729	85.646	0.9935
DES 19	-6.68862	2406.39782	80.369	0.9941
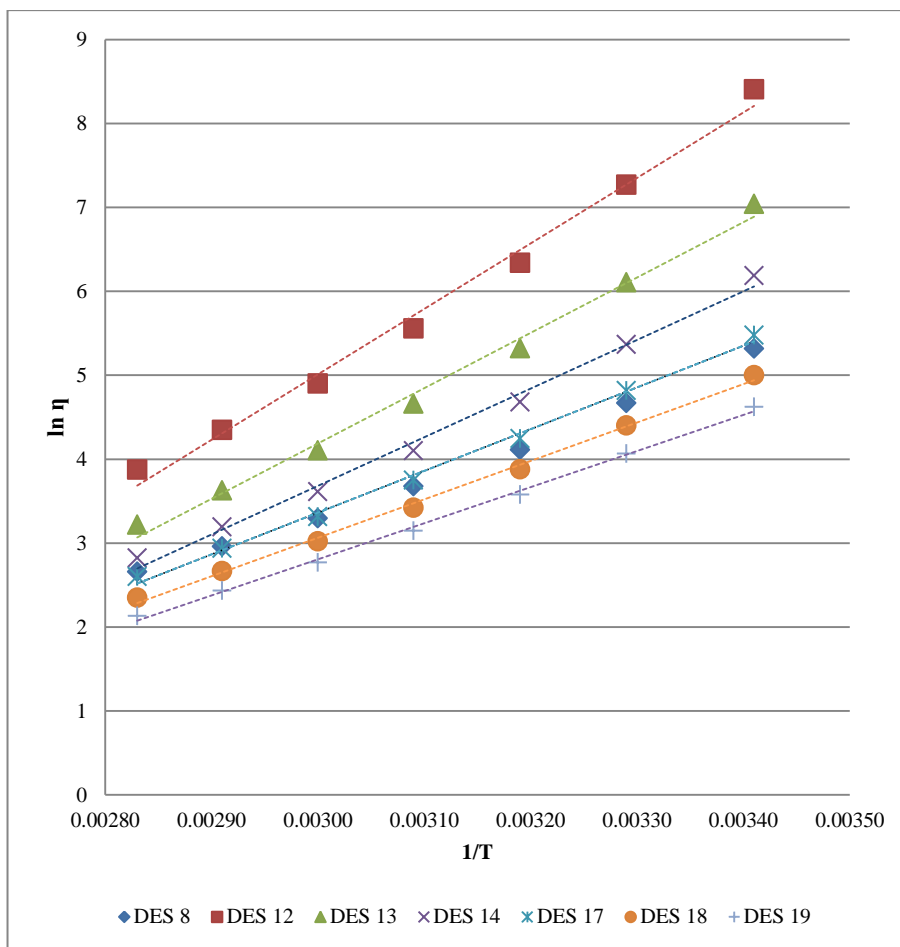
FIGURE 4.4   ln η against 1/T plot for all DES

4.3.3   Refractive Index

The refractive index is a dimensionless physical property which measures the bending of a ray of light when passing from one medium into another [61]. It is crucial property in many optical applications as it reflects the purity of solvent or concentration of components in a liquid. The refractive index of DESs samples have been measured as a function of temperature and are displayed in Figure 4.5 and Table 4.17 to 4.19. The result for all sample shows that the refractive index of DESs decrease with an increase of temperature and an increase of HBD content. This is because the density of the medium decreases, allowing more freedom for the movement of light. This translates into an increase in the speed of light in that medium and lower refractive index is observed. The data obtained are then plotted

into a graph to investigate the dependence of refractive index towards temperature, and fitting it through the Equation 8.

$$\eta = mT + c \qquad (8)$$

where η is refractive index of DES, T is temperature in Kelvin while m and c are the fitting parameters varied for different DESs. Table 4.20 shows the fitting parameters of density of each DES.

TABLE 4.17 Refractive Index versus Temperature Data for DES (6, 7 and 8) over the temperature range (298.15-328.15) K

T/K	DES 6	DES 7	DES 8
298.15	1.45487	1.45370	1.45252
303.15	1.45327	1.45279	1.45115
308.15	1.45230	1.45131	1.44973
313.15	1.45087	1.44979	1.44821
318.15	1.44944	1.44837	1.44679
323.15	1.44792	1.44680	1.44521
328.15	1.44650	1.44624	1.44366

TABLE 4.18 Refractive Index versus Temperature Data for DES (12, 13 and 14) over the temperature range (298.15-328.15) K

T/K	DES 12	DES 13	DES 14
298.15	1.45133	1.45047	1.44915
303.15	1.44894	1.44898	1.44800
308.15	1.44797	1.44779	1.44661
313.15	1.44696	1.44673	1.44520
318.15	1.44545	1.44501	1.44375
323.15	1.44393	1.44343	1.44203
328.15	1.44281	1.44211	1.44061

TABLE 4.19   Refractive Index versus Temperature Data for DES (17, 18 and 19) over the temperature range (298.15-328.15) K

T/K	DES 17	DES 18	DES 19
298.15	1.43738	1.43633	1.43562
303.15	1.43593	1.43479	1.43391
308.15	1.43458	1.43327	1.43289
313.15	1.43337	1.43197	1.43160
318.15	1.43187	1.43083	1.43014
323.15	1.43067	1.42950	1.42881
328.15	1.42930	1.42815	1.42750

TABLE 4.20   Result of Regression Analysis of Refractive Index versus Temperature Data for DES over the temperature range (298.15-328.15) K

DES	m	c	R^2
DES 6	-0.0014	1.4563	0.9977
DES 7	-0.0013	1.4552	0.9913
DES 8	-0.0015	1.4541	0.9995
DES 12	-0.0014	1.4522	0.9881
DES 13	-0.0014	1.4519	0.9964
DES 14	-0.0014	1.4508	0.9975
DES 17	-0.0013	1.4387	0.9995
DES 18	-0.0013	1.4375	0.9980
DES 19	-0.0013	1.4368	0.9981
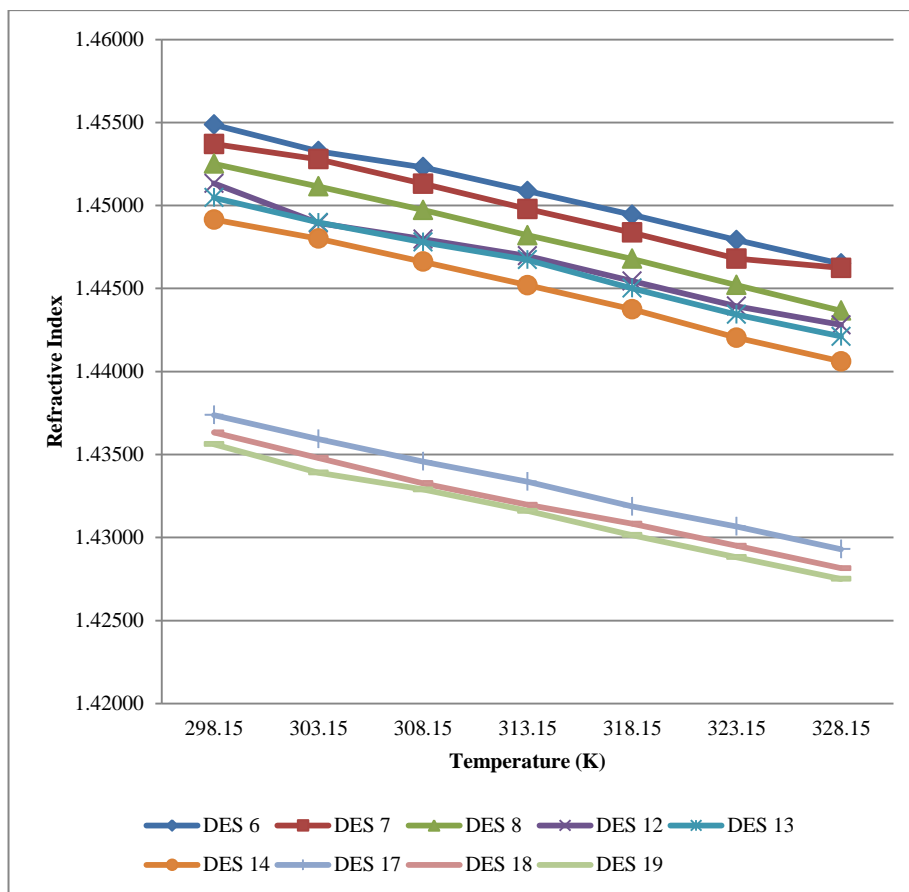
FIGURE 4.5   Refractive Index of DES against temperature range (298.15-328.15) K

4.4   Measurement of CO$_2$ Solubility

Solubility of CO$_2$ was measured using high pressure gas solubility cell. The solubility of CO$_2$ in DESs samples was measured at temperature 303.15 K in different pressure from 5 bar up to 20 bar. For the DESs prepared in this project, the solubility of CO$_2$ was estimated by using vapour-liquid equilibrium (VLE) data based on Peng-Robinson (PR) Equation of State (EoS) as defined in Equation 9. The equation was validated with the acquired experimental data and tested with other specific DESs described in the literature over an extensive range of temperature and pressure values [49].

$$P = \frac{RT}{v - b} - \frac{a}{v(v + b) + b(v - b)} \tag{9}$$

where *a* and *b* are functions of the critical properties of the chemical species as in the Equation 10 and 11.

$$a = 0.45724 \frac{(RT_C)^2}{P_C}[1 + m(1 - \sqrt{T_r})]^2 \qquad (10)$$

and

$$b = 0.0778 \frac{RT_C}{P_C} \qquad (11)$$

with

$$m = 0.37464 + 1.5422\omega - 0.2699\omega^2 \qquad (12)$$

The measurements of CO_2 solubility are given in Table 4.21 to Table 4.23 and Figure 4.6 to Figure 4.8 as a function of pressure. It can be observed that the solubility of CO_2 in the DESs increases as the pressure increases and HBD content increases. Such trends are usual for the solubility of gases in ILs and DESs. No literature comparison was accessible here because there is no data available yet on the solubility of CO_2 in the studied DESs.

TABLE 4.21   Solubility of CO_2 in DES 8 at 303.15 K

Pressure	DES 8 (mol/kg)
5 bar	0.2618
15 bar	0.4809
20 bar	0.6886

TABLE 4.22   Solubility of CO_2 in DES (12, 13 and 14) at 303.15 K

Pressure	DES 12 (mol/kg)	DES 13 (mol/kg)	DES 14 (mol/kg)
5 bar	0.0491	0.0521	0.0667
15 bar	0.5343	0.7030	0.8689
20 bar	0.7986	1.0728	1.3229

TABLE 4.23   Solubility of CO_2 in DES (17, 18 and 19) at 303.15 K

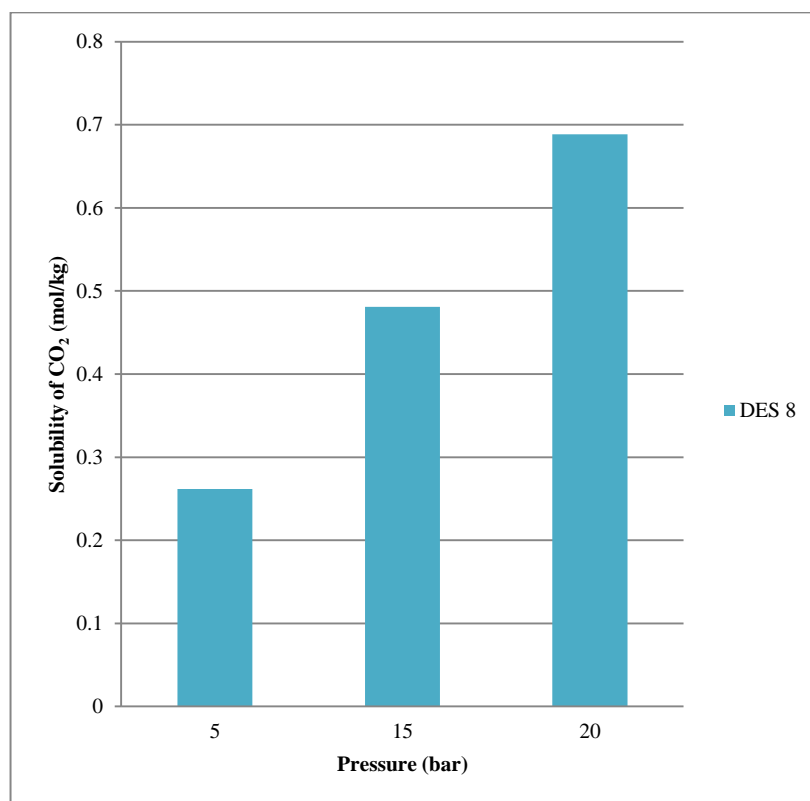| Pressure	DES 17 (mol/kg)	DES 18 (mol/kg)	DES 19 (mol/kg)
5 bar	0.2694	0.3776	0.4327
15 bar	0.6719	0.8479	0.9834
20 bar	0.9015	1.1205	1.3320

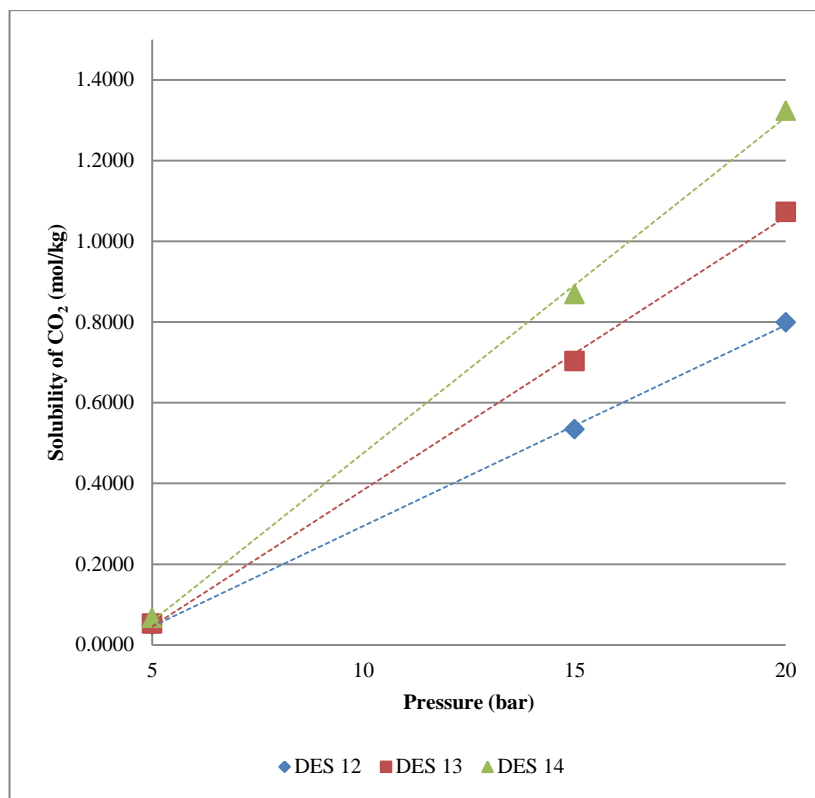FIGURE 4.6   Solubility of CO_2 as a function of Pressure in DES 8

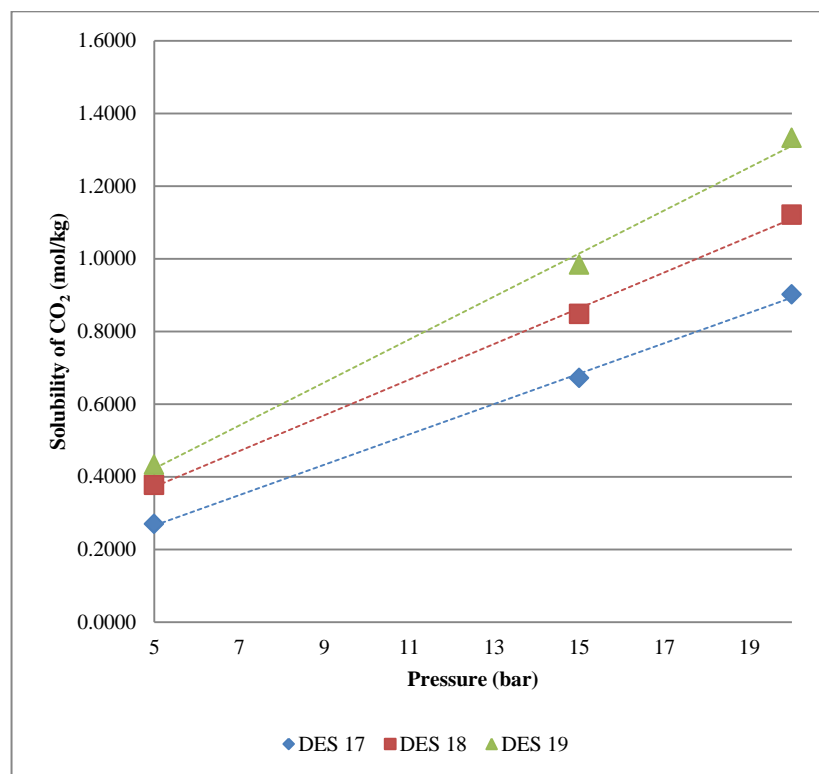FIGURE 4.7 Solubility of CO_2 as a function of Pressure for DES (12, 13 and 14)

FIGURE 4.8 Solubility of CO_2 as a function of Pressure for DES (17, 18 and 19)

CHAPTER 5

CONCLUSION AND RECOMMENDATION

5.1   Conclusion

Variety of new DESs is being synthesized and the prepared DESs are chosen based on the structure of salts and the HBD. The physical properties of DESs which is density, viscosity and refractive index and the thermal properties such as decomposition temperature and freezing point are being measured over temperature range of 293.15 K to 353.15 K at atmospheric pressure for the whole range of composition. Densities, viscosities and refractive index of sample formed decrease with an increase of temperature and an increase of HBD content. An empirical linear equation can be used to correlate density and refractive index as a function of temperature while VTF equation is used as fittings to the viscosity to correlate the dependence of viscosity towards temperature. The solubility of CO_2 in DESs will be measured in different molar ratios at the temperature of 303.15 K and pressure range from 5 bar up to 20 bar. The solubility of CO_2 using Peng-Robinson (PR) Equation of State (EoS) in the DESs increases as the pressure and HBD content increases.

5.2   Recommendation

1. To further conduct the CO_2 solubility test with new mixture of DESs and ternary deep eutectic solvents (TDESs).
2. To study the feasibility of having the DESs selected in the project in the oil and gas processing plant for CO_2 capture.

REFERENCES

[1]   A. Yamasaki, "An Overview of Mitigation Options for Global Warming & mdash; Emphasizing Sequestration Options," *Journal of Chemical Engineering of Japan*, vol. 36, pp. 361-375, 2003.

[2]   IPCC, "Climate Change 2007: Mitigation of Climate Change. Exit EPA Disclaimer Contribution of Working Group III to the Fourth Assessment Report of the Intergovernmental Panel on Climate Change," B. Metz, O.R. Davidson, P.R. Bosch, R. Dave, L.A. Meyer (eds). *Cambridge University Press, Cambridge, United Kingdom and New York, NY, USA,* 2007.

[3]   NRC, "Advancing the Science of Climate Change. Exit EPA Disclaimer National Research Council." *The National Academies Press, Washington, DC, USA,* 2010.

[4]   EPA, "Global Greenhouse Gas Emissions Data", 2013.

[5]   J.C.M. Pires, F.G. Martins, M.C.M. Alvim-Ferraz, M. Simões, "Recent developments on carbon capture and storage: an overview." *Chem. Eng. Res. Des.* 89, 1446–1460, 2011.

[6]   M. M. Abu-Khader, "Energy Sources Part A," 28, 1261, 2006.

[7]   S.M. Cohen, H.L. Chalmers, M.E. Webber, C.W. King. "Comparing post-combustion CO_2 capture operation at retrofitted coal-fired power plants in the Texas and Great Britain electric grids." *Environ. Res. Lett.* 6, 1–14,2011.

[8] C.B. Tarun, E. Croiset, P.L. Douglas, M. Gupta, M.H.M. Chowdhury. "Techno-economic study of CO_2 capture from natural gas based hydrogen plants." *Int. J. Greenhouse Gas Control* 1, 55–61, 2007.

[9] N. Dave, T. Do, G. Puxty, R. Rowland, P.H.M. Feron, M.I. Attalla. "CO_2 capture by aqueous amines and aqueous ammonia-a comparison." *Energy Procedia 1*, 949–954, 2006.

[10] N. Rodriguez, S. Mussati, N. Scenna. "Optimization of post-combustion CO_2 process using DEA-MDEA mixtures." *Chem. Eng. Res. Des.* 89, 1763–1773, 2011.

[11] M. Mofarhi, Y. Khojasteh, H. Khaledi, A. Farahnak. "Design of CO_2 absorption plant for recovery of CO_2 for flue gases of gas turbine." *Energy* 33, 1311–1319, 2008.

[12] M. Abu-Zahra, L.H. Schneides, J.P. Niederer, P.H. Feron, G.F. Versteeg. "CO_2 capture from power plants part I, parametric study of the technical performance based on monoethanolamine." *Int. J. Greenhouse Gas Control 1*, 37–46, 2007.

[13] M.K. Hanne, G.T. Rochelle. "Effects of the temperature bulge in CO_2 absorption from flue gas by aqueous monoethanolamine." *Ind. Eng. Chem. Res.* 47, 867–875, 2008.

[14] B.R. Anand, E.S. Rubin, D.W. Keith, M.G. Morgan. "Evaluation of potential cost reductions from improved amine-based CO_2 capture systems." *Energy Policy* 34,3765–3772, 2006.

[15] R. D. Rogers, K. R. Seddon. "Ionic liquids − Solvents of the future?" *Science* 302, 792−793, 2003.

[16] C. M. Clouthier, J. N. Pelletier. "Expanding the organic toolbox: A guide to integrating biocatalysis in synthesis." *Chem. Soc. Rev.* 41, 1585−1605, 2012.

[17] A. P. Abbott, G. Capper, D. L Davies, H. L. Munro, R. K. Rasheed, V. Tambyrajah. *Chem. Commun.* 2010.

[18] A. P. Abbott, D. Boothby, G. Capper, D. L. Davies, R. K. Rasheed. "Deep eutectic solvents formed between choline chloride and carboxylic acids: versatile alternatives to ionic liquids." *J Am Chem Soc*. 126: 9142–7, 2004.

[19] M. Avalos, R. Babiano, P. Cintas, J. L. Jimenez, J. C. Palacios. "Greener media in chemical synthesis and processing." *Angew Chem Int Ed*. 45: 3904–8, 2006.

[20] L. M. Galán Sánchez, G. W. Meindersma, A. B. de Haan. "Solvent properties of functionalized ionic liquids for CO_2 absorption." *Chem. Eng. Res. Des.* 85, 31–39, 2007.

[21] X. Li, M. Hou, B. Han, X. Wang, L. Zou. *J. Chem. Eng. Data*. 53, 548–550, 2008.

[22] M. Hasib-ur-Rahman, M. Siaj, F. Larachi. "Ionic liquids for CO_2 capture-Development and progress," *Chemical Engineering and Processing: Process Intensification,* vol. 49, pp. 313-322, 4//, 2010.

[23] P. J. Atkins, Physical Chemistry 8th edition.

[24] A. Yadav, S. Trivedi, R. Rai, S. Pandey, "Densities and dynamic viscosities of (choline chloride;glycerol) deep eutectic solvent and its aqueous mixtures in the temperature range (283.15–363.15)&0;K," *Fluid Phase Equilibria*. vol. 367, pp. 135-142, 4/15/, 2014.

[25] T. Welton. *Chem. Rev*. 99, 2071, 1999.

[26] P. Wasserscheid, T. Welton. "Ionic Liquids in Synthesis;" *Wiley-VCH: Weinheim*, 2008.

[27] A. Michel, F. Endres, D. R. MacFarlane, O. Hiroyuki, B. Scrosati. *Nat. Mater.* 8, 621, 2009.

[28] A. P. Abbott, I. Dalrymple, F. Endres, D. R. MacFarlane. "In Electrodeposition from Ionic Liquids;" *Wiley-VCH: Weinheim*. p1, 2008.

[29] J. S. Wilkes, M. J. Zaworotko. *Chem. Commun.* 965, 1992.

[30] F. Endres, S. Z. El Abedin. *Phys. Chem.* 8, 2101, 2006.

[31] L. Liu, Y. Kong. "Ionothermal synthesis of athree-dimensional zinc phosphate with DFT topology usingunstable deep-eutectic solvent as template-delivery agent.Micropor." *Mesopor. Mater.* 115, 624–628, 2008.

[32] C. A. Nkuku, R. J. LeSuer. "Electrochemistry in deep eutecticsolvents." *J. Phys. Chem.* B 111, 13271–13277, 2007.

[33] M. S. Sitze, E. R. Schreiter, E.V. Patterson, R.G. Freeman. *Inorg. Chem.* 40, 2298, 2001.

[34] A. P. Abbott, J. C. Barron, K. S Ryder, D. Wilson. *Chem. − Eur.J.* 13, 6495, 2007.

[35] M. Gambino, J. P. Bros. *Thermochim. Acta.* 127, 223, 1988.

[36] E. L. Smith, A. P. Abbott, and K. S. Ryder, "Deep Eutectic Solvents (DESs) and Their Applications," *Chem Rev*. 2014.

[37] A. P. Abbott, G. Capper, D. L. Davies, R. K. Rasheed, V. Tambyrajah. *Chem. Commun.* 70, 2003.

[38] A. P. Abbott, D. Boothby, G. Capper, D. L. Davies, R. J. Rasheed. *Am. Chem. Soc.* 126, 9142, 2004.

[39] R. Yusof, E. Abdulmalek, K. Sirat, M. Basyaruddin Abdul Rahman, "Tetrabutylammonium Bromide (TBABr)-Based Deep Eutectic Solvents (DESs) and Their Physical Properties," *Molecules,* 2014.

[40] C. Rub, B. Konig. "Low melting mixtures in organic synthesis — an alternative to ionic liquids?" *Green Chem.* 14, 2969–2982, 2012.

[41] R. B. Leron, D. S. H. Wong, M. H. Li, "Densities of a deep eutectic solvent based on choline chloride and glycerol and its aqueous mixtures at elevated pressures," *Fluid Phase Equilibria*, vol. 335, pp. 32-38, 12/15/, 2012.

[42] R. B. Leron, A. N. Soriano, M. H. Li, "Densities and refractive indices of the deep eutectic solvents (choline chloride&ethylene glycol or glycerol) and their aqueous mixtures at the temperature ranging from 298.15 to 333.15K," *Journal of the Taiwan Institute of Chemical Engineers.* vol. 43, pp. 551-557, 7//, 2012.

[43] P. G. Jessop, *Green Chem.* 13, 1391, 2011.

[44] J. O. Valderrama, W. S. Wilson, A. L. Juan. "Critical properties, normal boiling temperatures and acentric factor of 200 ionic liquids," *Ind. Eng. Chem. Res.* 47, 1318–1330, 2008.

[45] R. B. Leron, M. H. Li. "Solubility of carbon dioxide in a choline chloride–ethylene glycol based deep eutectic solvent." *Thermochim.* Acta 551, 14–19, 2013.

[46] R. B. Leron, M. H. Li. "Solubility of carbon dioxide in a eutectic mixture of choline chloride and glycerol at moderate pressures." *J. Chem. Thermodyn.* 57, 131–136, 2013.

[47] W. C. Su, D. S. H. Wong, M. H. Li. "Effect of water on solubility of carbon dioxide in (Aminomethanamide + 2-Hydroxy-N,N,N-trimethylethanaminium chloride)." *J. Chem. Eng.* Data 54, 1951–1955, 2009.

[48] G. N. Wang, Y. Dai, X. B. Hu, F. Xiao, Y. T. Wu, Z. B. Zhang, Z. Zhou. "Novel ionic liquid analogs formed by triethylbutyl ammonium carboxylate-water mixtures for CO_2 absorption." *J. Mol. Liq*. 168, 17–20, 2012.

[49] E. Ali, M. K. Hadj-Kali, S. Mulyono, I. Alnashef, A. Fakeeha, F. Mjalli, A. Hayyan. "Solubility of CO_2 in deep eutectic solvents: Experiments and modelling using the Peng–Robinson equation of state." *Chemical Engineering Research and Design.* 92, 1898–1906, 2014.

[50] R. B. Leron, A. Caparanga, M. H. Li, "Carbon dioxide solubility in a deep eutectic solvent based on choline chloride and urea at T 303.15–343.15 K and moderate pressures," *Journal of the Taiwan Institute of Chemical Engineers,* vol. 44, pp. 879-885, 11//, 2013.

[51] B. Jibril, F. M, J. Naser, Z. Gano, "New tetrapropylammnonium bromide-based deep eutectic solvents: synthesis and characterizations," *Journal of Molecular Liquids.* 462-469, 2014.

[52] Material Safety Data Sheet Potassium Carbonate MSDS

[53] Material Safety Data Sheet Sodium Acetate MSDS

[54] Material Safety Data Sheet Levulinic Acid MSDS

[55] Material Safety Data Sheet Ethylene Glycol MSDS

[56] F. M. J. Naser, B. Jibril, S. Al-Hatmi, and Z. Gano, "Potassium Carbonate as a Salt for Deep Eutectic Solvents," *International Journal of Chemical Engineering and Applications,* vol. 4, pp. 114-118, 2013.

[57] F. M., J. Naser, B. Jibril, S. Al-Hatmi, Z. Gano, "Ionic liquids analogues based on potassium carbonate," *Thermochimica Acta* 575 (2014) 135– 143, 2013.

[58] D. Choudhury, R. C. Borah, R. L. Goswamee, H. P. Sharmah, and P. G. Rao, "Non-isothermal thermogravimetric pyrolysis kinetics of waste petroleum refinery sludge by isoconversional approach," *Journal of Thermal Analysis and Calorimetry*, vol. 89, pp. 965-970, 2007/09/01 2007.

[59] L. F. Zubeir, M. H. M. Lacroix, and M. C. Kroon, "Low Transition Temperature Mixtures as Innovative and Sustainable CO_2 Capture Solvents," *The Journal of Physical Chemistry*, vol. 118, pp. 14429-14441, 2014/12/11 2014.

[60] Ramirez Verduzco, L.F. "Density and viscosity of biodiesel as a function of temperature: Empirical models." *Renew. Sustain. Enegy Rev*. 19, 652-665,2013.

[61] M. A. Kareem, F. S. Mjalli, M. A. Hashim, I. M. Al Nashef, *J. Chem. Eng. Data* 55, 4632-4637, 2010.

[62] Q. Zhang, K. de Oliveria Vigier, S., Royer, F.,Jerume, "Deep Eutectics Solvents: syntheses, properties and applications" *Chem. Soc. Rev*., 41, 7108-7146, 2012.

[63] C.Cadena, J.L. Anthony, J.K. Shah, T.L. Morrow, J.F. Brennecke, E.J. Maginn, "Why is CO_2 so soluble in Imidazolium-Based Ionic liquids?" *Journal American Chemical Society*, 2004.